UNIVERSITÉ DU QUÉBEC À MONTRÉAL

DYNAMIQUE DES GLACIERS VÊLANTS ET MÉCANISMES DE VÊLAGE D'ICEBERGS: LE CAS DE RINK ISBRÆ, GROENLAND

MÉMOIRE

PRÉSENTÉ

COMME EXIGENCE PARTIELLE

DE LA MAÎTRISE EN SCIENCES DE LA TERRE

PAR

DOROTA MEDRZYCKA

JANVIER 2015

REMERCIEMENTS

Thank you, first of all, to my supervisor Michel Lamothe. Michel, thank you for giving me the freedom to roam around and to complete this MSc program somewhat unconventionally, by spending most of the time away from Montreal, either on Svalbard or in Sweden.

I also thank Doug Benn, my project supervisor. Doug it was a great pleasure to work with you and I truly appreciate your feedback. Thank you for taking me on fieldwork on Paulabreen and organising the Kronebreen fieldwork, I had the best time.

I want to thank all who helped during fieldwork: Nick Hulton for heading out with me to install the first cameras at Kronebreen, and Heïdi Sevestre for retrieving the data and helping me out with all the small stuff afterwards. Thanks go to Jason Box for providing the new dataset from Rink Ibræ after the Kronebreen cameras failed, and to both Nick Hulton and Doug Benn for coordinating the project.

I spent quite a bit of time at Stockholm University (Institutionen för naturgeografi) where I was provided with access to a workspace (thank you Nina Kirchner) and plenty of coffee. Thank you to all at the department for your help.

Special thanks go to the family and friends who provided me with plenty of distractions in the form of additional fieldwork (Niels Weiss, Mark Allan), or trips (Niels Weiss, Ingeborg Pay, Mother and Father).

Funding was provided by the Fond de recherche du Québec – Nature et technologies (FQRNT) and the Faculté des sciences de l'UQAM. Field expenses were covered by the Arctic Field Grant (AFG) of the Research Council of Norway (RCN).

This work has lead me to one major realisation: with any given project, nothing ever goes according to plan.

TABLE DES MATIÈRES

LISTE DES FIGURES v

LISTE DES TABLEAUX vii

RÉSUMÉ viii

INTRODUCTION 1

CHAPITRE I
COMPORTEMENT DES GLACIERS VÊLANTS 6

1.1 Contrôles sur le processus de vêlage d'icebergs 6

1.2 Processus de vêlage d'icebergs 9

1.2.1 Taux de déformation longitudinale 9

1.2.2 Déséquilibre des forces au terminus 11

1.2.3 Vêlage sous-marin 14

CHAPITRE II
VARIABILITY IN CALVING BEHAVIOUR AT RINK ISBRÆ, WEST GREENLAND 15

2.1 Abstract 15

2.2 Introduction 15

2.3 Study site 17

2.4 Datasets and Methods 18

2.4.1 Timelapse cameras 18

2.4.2 Ice front mapping 19

2.4.3 Calving event magnitude scale 20

2.4.4 Surface air temperatures and Sea surface temperatures 21

2.5 Results 22

2.5.1 Front position change 22

2.5.2 Air and sea temperature 23

2.5.3 Ice mélange clearing date 24
2.5.4 Event size distribution 25
2.5.5 Calving styles and calving front geometry 27
2.6 Discussion 37
2.6.1 Melt-driven calving 37
2.6.2 Mechanically-driven calving 39
2.6.3 Ice mélange dynamics 41
2.7 Conclusion 45
CONCLUSION 47
RÉFÉRENCES 50

LISTE DES FIGURES

Figure		Page
0.1	Kronebreen, Svalbard	1
0.2	Nordenskiöldbreen, Svalbard	2
0.3	Camera et vue sur le terminus de Rink Isbræ, Groenland	4
1.1	Champ de crevasses	8
1.2	Schéma d'un front de vêlage	9
1.3	Kronebreen et Kongsvegen	10
1.4	Schéma des forces au terminus	12
2.1	Study site	18
2.2	Grid	20
2.3	Terminus position change	24
2.4	Event size distribution and mass loss	26
2.5	Magnitude of daily calving losses for 2007 and 2008	28
2.6	Magnitude of daily calving losses: 2009, 2010, and 2011	29
2.7	Magnitude of daily calving losses for all years	30
2.8	Spatial distribution of calving events	31
2.9	Pattern of surface crevasses	32
2.10	Calving front geometry after mélange clearing	32
2.11	Glacial meltwater upwellings	33
2.12	Notch at the waterline	34
2.13	Ice mélange	35

2.14 Magnitude 1 events 36

2.15 Calving pattern after mélange clearing 42

LISTE DES TABLEAUX

Tableau		Page
2.1	Dataset	19
2.2	Seasonal terminus position variations	23
2.3	Melt season and ice mélange clearing	25

RÉSUMÉ

Le processus de vêlage, c'est-à-dire la production d'icebergs par les glaciers s'écoulant dans l'eau, est un mécanisme d'ablation important. Dans le cas des glacies de marée, et particulièrement dans le cas des glaciers situés dans les hautes latitudes, le vêlage entraine des pertes de masse bien plus importantes que l'ablation par la fonte seule. En dépit de leur importance évidente, les interactions dynamiques entre le vêlage au terminus et les changements dans la dynamique du reste du glacier demeurent mal compris. Le présent mémoire traite de certaines questions concernant la complexité de la dynamique glaciaire des glaciers vêlants ("calving glaciers"), et examine la variabilité des processus de vêlage observés sur différents glaciers. Une étude de cas se concentrant sur Rink Isbræ, un important glacier émissaire sur la côte ouest du Groenland, démontre que deux styles de vêlage distincts agissent simultanément sur le même glacier. La variabilité dans le comportement de vêlage de Rink suggère que la production d'icebergs est le résultat d'une série de processus contrôlant l'ampleur, l'emplacement, ainsi que la périodicité des évènements de vêlage. La nature complexe des comportements de vêlage représente toujours un obstacle majeur à une évaluation précise de la sensibilité des glaciers de vêlage vis-à-vis les changements climatiques.

Mots-clés: vêlage, icebergs, glaciers émissaires, Groenland, dynamique glaciaire

INTRODUCTION

Les glaciers vêlants sont particuliers en raison du fait qu'ils se terminent dans l'eau et produisent des icebergs ce qui influence leur dynamique d'une manière fondamentale. La production d'icebergs est un mécanisme d'ablation dominant pour les glaciers de marée, et il est estimé être responsable d'environ 2/3 des pertes de masse de la calotte glaciaire du Groenland (Rignot and Kanagaratnam, 2006). Le vêlage représente donc une contribution majeure au flux d'eau douce vers les océans et joue un rôle clé dans les variations du niveau marin global (Rignot and Kanagaratnam, 2006). De nombreux glaciers vêlants, y compris dans l'Arctique, en Alaska, en Patagonie et en Antarctique, ont récemment connu une accélération rapide de leur écoulement, un amincissement et sont entrés en régression, résultant en une augmentation importante des taux de vêlage (ex. Arendt *et al.*, 2002; Rignot *et al.*, 2003; Cook *et al.*, 2005; Rignot and Kanagaratnam, 2006; Bamber *et al.*, 2007; Howat *et al.*, 2008; Rignot *et al.*, 2011).

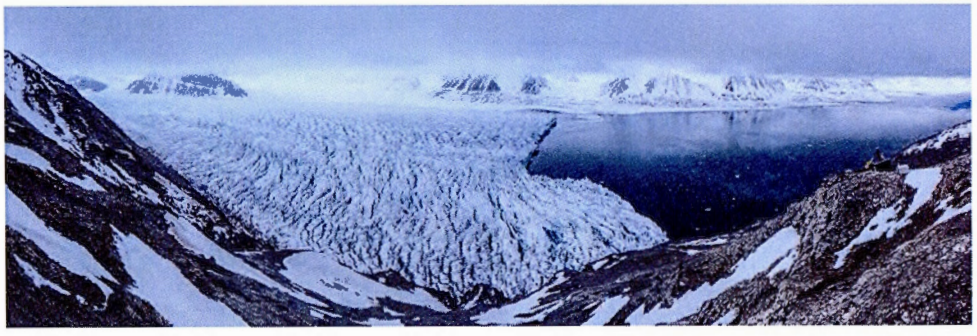

Figure 0.1 Kronebreen, un glacier de marée s'écoulant dans Kongsfjorden, Svalbard.

Malgré son importance évidente, la dynamique des glaciers vêlants et les mécanismes physiques contrôlant le taux de vêlage restent toujours mal compris. L'état actuel des connaissances est limité par les défis associés à l'acquisition de données sur le terrain étant donné que les sites sont souvent situés dans des environnements difficiles d'accès. La plupart des études sont menées sur un petit

nombre de glaciers bien étudiés (ex. Columbia Glacier, Alaska (ex. Post, 1975; Brown *et al.*, 1982; Meier *et al.*, 1985; Krimmel, 2001) et Jacobshavn Isbræ, côte ouest du Groenland (ex. Sohn *et al.*, 1998; Joughin *et al.*, 2004; Thomas, 2004; Luckman and Murray, 2005)), et les observations recueillies à ces quelques sites ne peuvent pas être extrapolées aux glaciers situés dans d'autres régions (Carr *et al.*, 2013). Cela est particulièrement le cas compte tenu de la grande variété de glaciers vêlants autour du monde. En fonction de leur emplacement, ceux-ci peuvent présenter un régime thermique froid et/ou tempéré, et leur termini peuvent soit être à flot et se terminer en une langue de glace flottante, ou être ancré sur le lit. Leur comportement dépend aussi s'ils se terminent dans les eaux de mer (glaciers de marée), ou dans les lacs proglaciaires (glaciers d'eau douce) (Meier and Post, 1987). Le large éventail de comportements (ou métabolismes) des glaciers de vêlage constitue un obstacle au développement d'un modèle de vêlage universel capable d'expliquer tous les processus observés (Benn *et al.*, 2007b; Bassis, 2011).

Figure 0.2 Falaises terminales de Nordenskiöldbreen, dans Billefjorden, Svalbard.

Les glaciers sont généralement considérés comme de bons indicateurs des changements climatiques car les fluctuations de longueur et de la position de la marge glaciaire sont influencées par les variations du bilan de masse (Oerlemans, 2005). Cependant, les glaciers couverts de débris, les glaciers connaissant des périodes

de crue, ainsi que les glaciers vêlants présentent souvent un comportement atypique qui peut être dissocié des fluctuations climatiques. Les glaciers vêlants sont connus pour subir des cycles d'avancées lentes, suivies de retraits rapides dus à la désintégration du terminus par le vêlage (Post, 1975; Meier and Post, 1987; Post *et al.*, 2011). Ce comportement instable suggère que la relation entre le vêlage et les forçages climatiques est complexe, et que la dynamique interne glaciaire ainsi que des facteurs spécifiques à chaque glacier ont une influence cruciale sur les fluctuations de longueur des glaciers (Carr *et al.*, 2013). Comme décrit à l'origine par Post (1975), le cycle des glaciers de marée était considéré comme opérant sur des échelles de temps millénaires. Les avancées (~100-1,000 ans) et les reculs (~10-100 ans) étaient donc traités comme une réponse (avec un certain délai) aux fluctuations climatiques à long terme (Post, 1975; Meier and Post, 1987). De nouveaux développements dans les deux dernières décennies ont abouti à une meilleure compréhension des conditions au terminus, c'est-à-dire l'interface entre l'océan et la glace, et ont révélé un couplage important entre les facteurs atmosphériques/océaniques, la présence de glace de mer au terminus, et la dynamique de vêlage (Carr *et al.*, 2013). Des études récentes indiquent que les glaciers de marée peuvent subir des changements rapides sur des périodes courtes de quelques années, en réponse à un certain nombre de forçages environnementaux externes à court terme (Joughin *et al.*, 2004, 2008b, 2012; Howat *et al.*, 2007, 2008; Rignot *et al.*, 2010; Straneo *et al.*, 2010; Howat and Eddy, 2011; Nick *et al.*, 2013).

Le détachement d'icebergs est essentiellement un processus en deux parties impliquant la propagation de fractures et la séparation de blocs de glace de la masse principale du glacier (Figure 0.2) (Bassis and Jacobs, 2013). Il est donc fortement couplé à la dynamique glaciaire et à l'équilibre de forces au terminus. La difficulté d'établir un lien clair entre les évènements de vêlage individuels et des facteurs déclencheurs spécifiques souligne la nature complexe des processus de vêlage. En d'autres termes, les évènements de vêlage peuvent résulter de multiples forçages agissant à la fois localement et globalement, et sur des échelles de temps courtes et longues (Benn *et al.*, 2007b). Les contrôles potentiels affectant le comportement des glaciers vêlants comprennent les facteurs spécifiques à chaque glacier, tels que l'épaisseur de la marge et la topographie du fjord, ainsi que les facteurs externes liés aux conditions atmosphériques et océaniques, autant locales qu'à

grande échelle. L'importance relative et les relations entre les différents forçages sont encore mal connues, et varient souvent selon le glacier et l'échelle de temps considérée. Cela pose un obstacle majeur à la formulation d'une évaluation précise de la sensibilité des glaciers vêlants aux changements climatiques (Bamber *et al.*, 2007; Carr *et al.*, 2013).

Figure 0.3 Camera et vue sur le terminus de Rink Isbræ.

Le présent mémoire se concentre sur cette question et examine le rôle des différents mécanismes qui contrôlent le moment, l'emplacement et l'ampleur des évènements de vêlage, afin d'améliorer notre compréhension des divers mécanismes pouvant contrôler le comportement des glaciers de marée. Le premier chapitre présente une synthèse de la littérature actuelle sur le comportement des glaciers vêlants incluant les contrôles sur le vêlage, ainsi que la gamme de processus conduisant au détachement d'icebergs. Le second chapitre est une étude de cas, présentant la variabilité des comportements liés au vêlage observés à Rink Isbræ, un important glacier émissaire sur la côte ouest du Groenland. L'étude utilise des données visuelles fournies par un système de caméra digitale (Figure 0.3) installée par Dr. Jason Box (Geological Survey of Denmark and Greenland, GEUS) dans le cadre du Extreme Ice Survey (EIS), et consiste en une analyse de l'activité au front du

glacier sur une période de cinq ans (2007-2011).

Ce chapitre sous forme d'article est présentement en préparation pour soumission à une revue scientifique, avec comme second auteur, Dr. Doug Benn (University Centre in Svalbard, UNIS), superviseur du projet de maîtrise duquel résulte ce mémoire. Le chapitre, intitulé "Variability in calving behaviour at Rink Isbræ, west Greenland" comporte une introduction détaillée au sujet traité. Les références pour tous les chapitres sont présentées ensemble à la fin du mémoire.

CHAPITRE I

COMPORTEMENT DES GLACIERS VÊLANTS

1.1 Contrôles sur le processus de vêlage d'icebergs

La dynamique des glaciers vêlants est sensible aux conditions à l'interface entre la glace et l'océan dans lequel ils terminent. La présence d'eau au terminus influence l'équilibre de forces et a un impact majeur sur la résistance à l'écoulement à la base du glacier, et donc sur la vélocité de la glace, en particulier là où la profondeur de l'eau est suffisamment importante pour forcer le terminus à se soulever du à la poussée d'Archimède. Le terminus devient à flot si l'épaisseur de la glace est moindre qu'une épaisseur critique, ou l'épaisseur de flottaison, H_F:

$$H_F = \frac{\rho_W}{\rho_I} D_W \tag{1.1}$$

où D_W est la profondeur de l'eau et ρ_i et ρ_w sont la densité de la glace et de l'eau respectivement. Bien que la densité de la glace reste constante ($\sim$ 900 kg m $^{-3}$), la densité de l'eau varie (Benn and Evans, 2010). Cela signifie que l'épaisseur de flottaison est plus faible dans l'eau douce ($\rho_w \sim 1000$ kg m^{-3}) que dans l'eau de mer ($\rho_w \sim 1{,}030$ kg m^{-3}) en raison de la différence de densité, dépendant de la salinité (Benn and Evans, 2010).

Le taux de vêlage d'icebergs, U_C, peut être défini comme la différence entre la vitesse à laquelle la glace est acheminée au front du glacier et le taux de changement de position du terminus:

$$U_C = \bar{U}_T - \frac{\delta L}{\delta t} \tag{1.2}$$

où $\bar{U}_T$ est la vitesse moyenne d'écoulement de la glace, L est la longueur du glacier, et t est le temps (Benn *et al.*, 2007a). Cette relation ente le taux de vêlage, l'écoulement de la glace, et la position du terminus peut être considérée de deux manières distinctes.

La première approche se concentre sur les contrôles sur les taux de vêlage et la vitesse de la glace, et les changements de position du terminus sont considérés comme le résultat d'un déséquilibre entre ces deux facteurs. Dans cette perspective, le taux de vêlage est contrôlé par des variables environnementales indépendantes. Basé sur des observations sur un certain nombre de glaciers de marée en Alaska, Brown *et al.* (1982) ont proposé une connexion entre la profondeur de l'eau, D_W, au terminus et le taux de vêlage, U_C:

$$U_C = a + bD_W \tag{1.3}$$

où a et b sont tous deux des coefficients déterminés empiriquement (Benn *et al.*, 2007a). Plusieurs études ont vérifié cette relation notant que le terminus devient instable lorsqu'il entre en contact avec des eaux profondes (Post, 1975; Pelto and Warren, 1991; Hanson and Hooke, 2000; Skvarca *et al.*, 2003). D'autres ont trouvé que ce modèle ne pouvait pas expliquer tous les comportements de vêlage observés étant donné que la relation entre le taux de vêlage et la profondeur de l'eau ne s'applique pas à tous les glaciers de marée et en tout temps (van der Veen, 1996, 2002).

La seconde approche se concentre sur la position de terminus et sur la vélocité du glacier et considère le taux de vêlage comme un résultat secondaire de la dynamique glaciaire (van der Veen, 1996, 1997b, 2002; Vieli *et al.*, 2001, 2002). Meier and Post (1987) ont suggéré un lien entre le taux de vêlage et la pression effective (différence entre la pression de couverture de la glace, et la pression de l'eau à la base) à la base du glacier. Cette perspective prévoit que le glacier devrait se retirer vers une position où la pression effective à la base tend vers zéro et le glacier entre en flottaison. Van der Veen (1996, 1997b) a développé cette idée en incorporant la profondeur de l'eau et à proposé un nouveau critère qu'il a nommé "height above buoyancy". Ce critère suggère que le glacier a tendance à reculer vers une position où la hauteur totale du terminus atteint une valeur critique

(~50 m) au dessus de son épaisseur de flottaison. Une variation à ce critère a été proposé par Vieli *et al.* (2001, 2002) où la valeur fixe de 50 m est remplacée par une fraction donnée de l'épaisseur de flottaison. Une limitation importante de ce critère est qu'il ne tient pas compte des platesformes et des langues de glace flottantes, car il ne permet pas au terminus de s'amincir au delà de l'épaisseur de flottaison sans se désintégrer en morceaux (Benn *et al.*, 2007a,b).

Figure 1.1 Champ de crevasses à Kronebreen, Svalbard.

Afin de répondre aux lacunes des modèles précédents Benn *et al.* (2007a,b) ont proposé un critère de vêlage basé sur la profondeur des crevasses qui prédit la position du terminus en considérant le taux de contraintes longitudinales près du front du glacier (Figure 1.1). Ce critère indique que le détachement d'icebergs se produit lorsque le régime extensif est suffisant pour que les crevasses puissent se propager vers le bas, à travers la glace, pour atteindre le niveau de l'eau (Benn *et al.*, 2007a,b), ou, comme l'ont ensuite proposé Nick *et al.* (2010) pour que les crevasses se propagent à travers toute l'épaisseur du glacier. L'emplacement, la magnitude, et le moment du détachement d'icebergs dépendent donc tous de la propagation de fractures qui reflète l'état de stress de la glace, et qui dicte la position et la géométrie du front glaciaire.

1.2 Processus de vêlage d'icebergs

La propagation de fractures se produit en réponse à de multiples mécanismes de forçage, et le vêlage est probablement le résultat d'une série de processus (Figure 1.2). Benn *et al.* (2007b) ont identifié trois ordres de processus de vêlage capables de générer des contraintes suffisantes pour provoquer la propagation de fracture et le détachement d'icebergs: (1) le taux de déformation longitudinale (ou l'allongement du glacier), (2) le déséquilibre des forces au front glaciaire, et (3) le vêlage sous-marin.

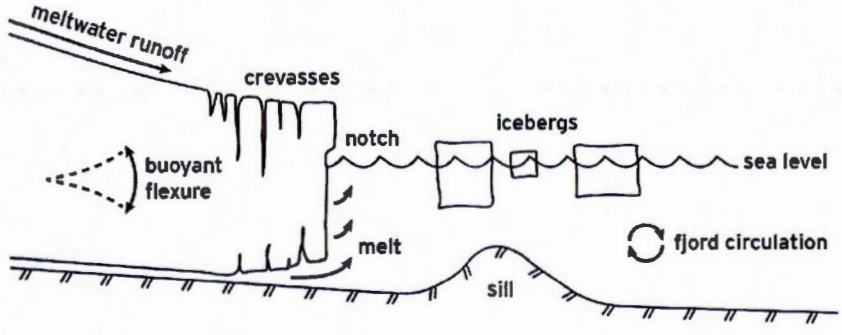

Figure 1.2 Schéma d'un front de vêlage et les processus opérant à l'interface entre la glace et l'océan (d'après W.T. Pfeffer, communication personnelle).

1.2.1 Taux de déformation longitudinale

La structure de vitesse d'écoulement du glacier est déterminée par la répartition spatiale des contraintes, notamment le "driving stress" et le "resistive stress". Les gradients de stress longitudinaux se développent en réponse à la résistance au glissement, à la base du glacier et au marges latérales. La vitesse d'écoulement a tendance à augmenter vers le terminus alors que le glacier devient à flot, du à une réduction de la pression effective et une résistance au glissement moindre. La résistance au glissement est donc affectée par la présence d'eau au front, ainsi que par l'épaisseur du glacier. Ceci implique des vitesses plus élevées, plus la langue de glace est mince, et plus l'eau est profonde (Meier and Post, 1987; Vieli *et al.*, 2000; O'Neel *et al.*, 2001, 2005; Vieli *et al.*, 2004; Howat *et al.*, 2007, 2008). La résistance au glissement aux marges latérales est d'un autre côté inversement proportionnelle

à la largeur de la vallée glaciaire, et la vitesse a tendance à augmenter lorsque le fjord s'élargit. Là où la résistance au glissement à la base est faible, la résistance latérale peut contribuer de manière significative à l'équilibre des forces. Ceci peut donc stabiliser le terminus et lui fournir la résistance nécessaire pour former un langue de glace flottante (Benn *et al.*, 2007a). Les gradients de stress longitudinaux dépendent également des conditions aux falaises au front et au transfert de "backstress". Van der Veen (1997a) définit le "backstress" comme le transfert, par les gradients de stress longitudinaux, de la résistance à l'écoulement à la base et aux marges latérale, vers l'amont du glacier. Là où les plateformes et les langues glaciaires flottantes sont contraintes par la topographie, la perte d'une portion de la glace flottante résulte en une réduction de "backstress" qui peut causer une accélération en amont du terminus (Benn *et al.*, 2007b). La structure de vitesse du glacier dépend donc de la distribution spatiale de la pression effective, de la largeur de la vallée, ainsi que des gradients de stress longitudinaux.

Figure 1.3 Kronebreen (bas gauche) et Kongsvegen (haut droit), Kongsfjorden, Svalbard. Les deux glaciers se joignent à 5 km du terminus et présentent des régimes extensifs très différents. Kronebreen est fortement crevassé alors que Kongsvegen a une surface plus régulière.

Les gradients de stress longitudinaux sont aussi influencés par la présence d'un

mélange de glace, ou "ice mélange", au front du glacier. Ce mélange de glace se forme en hiver et consiste en une masse semi-rigide formée de glace de mer et d'icebergs qui est poussé dans le fjord à la vitesse d'avancée du terminus. Le mélange agit essentiellement comme une mince langue de glace transitoire et peut générer une petite force résistive qui stabilise le front et limite le vêlage (Sohn *et al.*, 1998; Joughin *et al.*, 2008c; Amundson *et al.*, 2010; Howat *et al.*, 2010; Reeh *et al.*, 2001; Herdes *et al.*, 2012; Cassotto *et al.*, 2015). Le vêlage reprend alors que le mélange s'affaiblit à la fin de l'hiver et diminue progressivement à la fin de l'été alors que la consolidation de la glace de mer résulte en l'accumulation progressive du "backstress" (Sohn *et al.*, 1998). La présence de glace de mer dans le fjord a donc une influence majeure sur la production d'icebergs et contribue aux avancées et reculs saisonniers (Sohn *et al.*, 1998; Joughin *et al.*, 2008c; Amundson *et al.*, 2010).

Lorsque les contraintes d'extension sont suffisamment importantes pour initier le processus de fracturation, des crevasses transverses se propagent à travers la glace (Figure 1.3). De même, lorsqu'elles sont soumises à des forces supplémentaires, les crevasses préexistantes, advectées des régions de stress élevé en amont, peuvent aussi conduire au détachement d'icebergs (Bassis and Jacobs, 2013). L'introduction d'eau de fonte ou de pluie dans les crevasses de surface est un facteur additionnel pouvant renforcer la fracturation. L'action de l'eau a comme effet d'augmenter la pression dans les fractures et peut potentiellement forcer les crevasses à se propager à travers toute l'épaisseur du glacier ou de la plateforme flottante (van der Veen, 1998, 2007; Scambos *et al.*, 2000; MacAyeal *et al.*, 2003; Cook *et al.*, 2012). Le taux de déformation longitudinale qui détermine l'emplacement et la profondeur des crevasses, ainsi que l'épaisseur de la glace au terminus qui décide de la facilité d'une crevasse à pénétrer jusqu'à la base du glacier, représentent ensemble le contrôle primaire sur les variations de position du terminus (Benn *et al.*, 2007a,b).

1.2.2 Déséquilibre des forces au terminus

Le déséquilibre des forces agissant localement aux falaises de glace terminales représente un processus de second ordre, superposé sur la structure de vélocité du

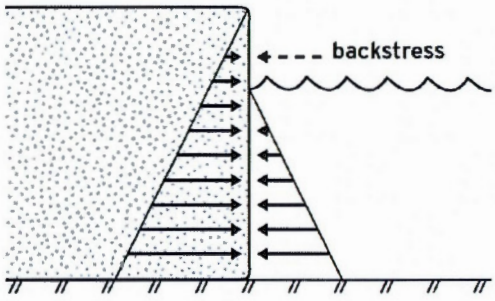

Figure 1.4 Schéma des forces cryostatiques (gauche) et hydrostatiques (droite) au terminus. Un "backstress" supplémentaire peut être fourni par la présence d'un mélange de glace dans le fjord (modifié à partir de (Benn *et al.*, 2007b)).

glacier. Les gradients de stress sont déterminés par l'interaction entre la pression cryostatique de la glace agissant vers l'aval, et la pression hydrostatique de l'eau qui pousse vers l'amont (Figure 1.4). En dessous du niveau de l'eau, la pression cryostatique est partiellement opposée par la force hydrostatique. Cependant, la partie subaérienne de la falaise de glace est pratiquement innoposée par la pression atmosphérique (Benn *et al.*, 2007b). Les gradients de stress sont plus importants plus les falaises sont hautes, et la pression cryostatique augmente progressivement vers le bas pour atteindre un maximum au niveau de l'eau (Hanson and Hooke, 2000). Les contraintes extensives qui résultent de cette pression peuvent conduire à la propagation de fractures.

Le déséquilibre de force au terminus est potentiellement amplifié par l'érosion thermique résultant de la fonte au niveau, ou sous le niveau d'eau. La fonte sous-marine peut causer un surcreusement de la partie submergée et former un surplomb (Benn *et al.*, 2007b). Bien que le taux de fonte augmente avec la température de l'eau, le processus de convection induit par l'écoulement des eaux de fonte glaciaire vers le fjord joue un rôle crucial en renforçant la circulation sous-marine. La convection agit comme une pompe et assure l'arrivée des eaux marines relativement chaudes vers les falaises terminales, favorisant ainsi la fonte (Motyka *et al.*, 2003, 2011; Jenkins, 2011). Lorsque les taux de fonte subaquatiques dépassent ceux de la partie subaérienne, le développement de surplombs améliore

encore le déséquilibre de force aux falaises de glace. Ceci conduit au basculement vers l'avant de blocs de glace et éventuellement au détachement d'icebergs (Theakstone and Knudsen, 1986; Kirkbride and Warren, 1997; Vieli *et al.*, 2002; Haresign and Warren, 2005). Dans certain cas, les taux de vêlage sont directement contrôlés par la vitesse d'érosion thermique et de surcreusement des falaises terminales (Röhl, 2006; Dykes *et al.*, 2010).

Les termini flottants sont aussi soumis à la force d'Archimède qui impose un torque sur la langue de glace à la jonction entre la section flottante et le reste du glacier sur terre. Un amincissement additionnel du terminus augmente le déséquilibre avec la pression hydrostatique et la glace devient à flot (Warren *et al.*, 2001; Benn *et al.*, 2007b). En raison de la différence de densité de l'eau, l'épaisseur de flottaison est plus élevée dans l'eau de mer que dans l'eau douce et, pour une épaisseur donnée, les glaciers de marée subissent une flexion supérieure aux glaciers lacustres. En réponse à la force d'Archimède, la langue de glace flottante peut devenir soulevée et inclinée vers l'arrière. La rupture se produit le long des lignes de faiblesse fournies par les crevasses préexistantes advectées de l'amont glaciaire (Benn *et al.*, 2007b).

L'accroissement progressif des forces de flexion vers le haut peut être accommodé par la déformation interne de la glace, mais les perturbations plus rapides sont plus susceptibles de conduire à la propagation de fractures et au vêlage (Boyce *et al.*, 2007). Benn *et al.* (2007b) ont proposé que les taux de contraintes longitudinales sont le contrôle primaire sur la position du terminus car ils déterminent les limites de la marge glaciaire en déterminant l'emplacement des crevasses. Le déséquilibre de forces au terminus représente un contrôle secondaire car il sape davantage l'intégrité du front et peut causer le glacier à se retirer. Toutefois, lorsque les vitesses de déformation longitudinales sont faibles, la position du terminus peut être contrôlée directement par les processus secondaires. Malgré l'importance primordiale de la structure de vitesse du glacier dans le contrôle du processes de vêlage, il n'y a pas de relation directe entre les taux de déformation longitudinale et les taux de vêlage. Les processus décrits ci-dessus représentent les contrôles sur l'emplacement et la magnitude des événements de vêlage individuels, mais pas sur les taux de vêlage eux-mêmes (Benn *et al.*, 2007b).

1.2.3 Vêlage sous-marin

Le vêlage sous-marin peut être considéré comme un contrôle de troisième ordre car il dépend des processus de premier et second ordre (Benn *et al.*, 2007b). Les sections submergées des falaises de glace, ou ce qu'on appelle des pieds de glace ("ice foot"), se forment en réponse à la fonte au niveau de l'eau, ou au vêlage de la partie subaérienne de la marge (Warren *et al.*, 1995; Kirkbride and Warren, 1997; Motyka, 1997; Vieli *et al.*, 2002; O'Neel *et al.*, 2007). La perte soudaine de la pression de couverture de la glace sur le pied de glace submergé entraine le déséquilibre des forces et peut causer le détachement de la partie sous-marine. Les icebergs qui résultent de ce processus jaillissent vers la surface et émergent parfois à des distances considérables du front de glace (Motyka, 1997).

CHAPITRE II

VARIABILITY IN CALVING BEHAVIOUR AT RINK ISBRÆ, WEST GREENLAND

2.1 Abstract

Iceberg calving is a sporadic process with a large variability in the magnitude, location, and timing of events. Calving styles range from the periodic breakup of large full-thickness tabular icebergs from floating ice tongues, to the more frequent capsizing of small blocks detaching above the waterline. The diversity in calving behaviours observed at marine-terminating glaciers points to the fact that iceberg production is the result of a series of different processes, and the precise mechanisms responsible remain largely unknown. This study presents detailed observations of calving behaviour variability from daily photographs acquired over a five year period (2007-2011) over the terminus of Rink Isbræ, west Greenland. The evidence suggests that calving at Rink is characterised by two distinct styles with different temporal and spatial footprints. It is suggested that at least two (sets of) mechanisms are controlling calving variability at this location, namely (1) melt-driven processes enhancing submarine undercutting and (2) mechanically-driven buoyant flexure. As the second mechanism is responsible for most of the mass lost through calving at Rink, it could potentially represent an important control on the stability of other Greenland glaciers as well.

2.2 Introduction

Recent studies indicate that the dynamics of marine-terminating glaciers are sensitive to changes in boundary conditions at the terminus. Feedbacks between

calving and ice dynamics imply a strong coupling between processes acting at the ice margins and changes upglacier (Joughin *et al.*, 2004; Thomas, 2004; Howat *et al.*, 2005; Joughin *et al.*, 2008c; Nick *et al.*, 2009; Vieli and Nick, 2011). Studies focusing on individual calving events suggest that rapid and localised perturbations may additionally determine the location, magnitude, and timing of events (O'Neel *et al.*, 2003, 2005, 2007; Bassis and Jacobs, 2013; Chapuis and Tetzlaff, 2014). Short-term terminus stability is therefore dependent on several parameters modifying boundary conditions at the ice cliffs, including both atmospheric and oceanic factors, the presence of sea ice/ice mélange in the fjord, as well as glacier specific factors such as ice thickness and fjord bathymetry. For this reason, and due to the wide range of calving styles observed at marine-terminating glaciers, there is no universal law that would adequately explain all calving behaviour. The mechanisms controlling the variability in calving behaviour, including at the interannual, seasonal, and single-event scale, remain largely unknown.

Calving is a sporadic process and consists of fracture propagation and the detachment of icebergs from the terminal ice cliffs following terminus destabilisation (Bassis and Jacobs, 2013). Calving styles and iceberg aspect ratio are therefore primarily controlled by longitudinal stress gradients within the glacier which determine the location and depth of transverse crevasses (Benn *et al.*, 2007a; Nick *et al.*, 2010). Variations in buoyancy conditions at the terminus further alter the force balance and can push the ice margin out of equilibrium, and promote calving (Benn *et al.*, 2007b). Several mechanisms have been proposed as having an impact on calving by modifying the force balance at the terminus. Longitudinal stress gradients can be influenced by variations in backstress resulting from the presence of a proglacial ice mélange in the fjord during the winter, which provides a small resistive force, stabilises the terminus and suppresses calving (Amundson *et al.*, 2010; Vieli and Nick, 2011). Additionally, the presence of water in surface crevasses can promote calving by causing the fractures to deepen and produce icebergs (Benn *et al.*, 2007a; Nick *et al.*, 2010; Vieli and Nick, 2011; Cook *et al.*, 2012). Buoyancy conditions can be affected by submarine melt and undercutting of the terminus which modifies the stress balance at the ice cliffs and promotes calving (Motyka *et al.*, 2003; O'Leary and Christoffersen, 2013).

This study aims to identify the different mechanisms affecting calving behaviour variability at Rink Isbræ, a major outlet glacier in west Greenland. Individual calving events were documented from a dataset of daily terrestrial photographs acquired over the span of five years (2007-2011) by the Extreme Ice Survey (EIS). A qualitative assessment of calving behaviour was compiled including information concerning the relative magnitude, timing and location of single calving events, in order to determine the controls on event size, inter-event intervals, as well as any spatial patterns in calving activity. The temporal evolution of terminus geometry indicates that Rink Isbræ exhibits two distinct calving styles including the sporadic detachment of large full-thickness km-sized tabular icebergs, and the more frequent capsizing of smaller bergs and slabs. The variability in calving behaviour is shown to depend on the interplay between longitudinal stresses and buoyancy conditions at the terminus. More specifically, small events occur more frequently in response to melt-driven processes, whereas the large ones are mechanically-driven and result from buoyant flexure at the terminus.

2.3 Study site

Rink Isbræ (71°45'N, 51°40'W) terminates in a narrow fjord in the Uummannaq district on the west coast of Greenland (Figure 2.1). With a drainage basin size of 30,000 km^2, it drains ~3.5% of the Greenland ice sheet (Rignot and Kanagaratnam, 2006) through a 4.5 km wide terminus. The front position remained relatively stable over the 2000-2010 period (Howat *et al.*, 2010; Box and Decker, 2011) and discharge rates of 11.8 $km^3\ a^{-1}$ of ice were measured between 2000 and 2005 (Rignot and Kanagaratnam, 2006). No speedup or surface elevation changes were recorded between 2000 and 2009 (McFadden *et al.*, 2011). Ice flow speed variations are correlated with seasonal terminus position changes and surface velocities vary by approximately 25%, ranging between 10 and 12.5 m d^{-1} (Howat *et al.*, 2010).

Bathymetric data of the inner fjord reveals two deep basins reaching over 1000 m below water level, separated by a 200 m high submarine moraine ridge, peaking at roughly 600 m below water level, and extending across the fjord about 2 km from the ice margin (Dowdeswell *et al.*, 2014). The maximum depth of the ice

at the glacier front is estimated to reach ~750 m in the midsection of the fjord (Chauché *et al.*, 2014). Although there is no detailed data of ice thickness at the terminus, the fact that Rink Isbræ produces large full-thickness tabular icebergs indicates that the terminus may be close to floatation (Ahn and Box, 2010).

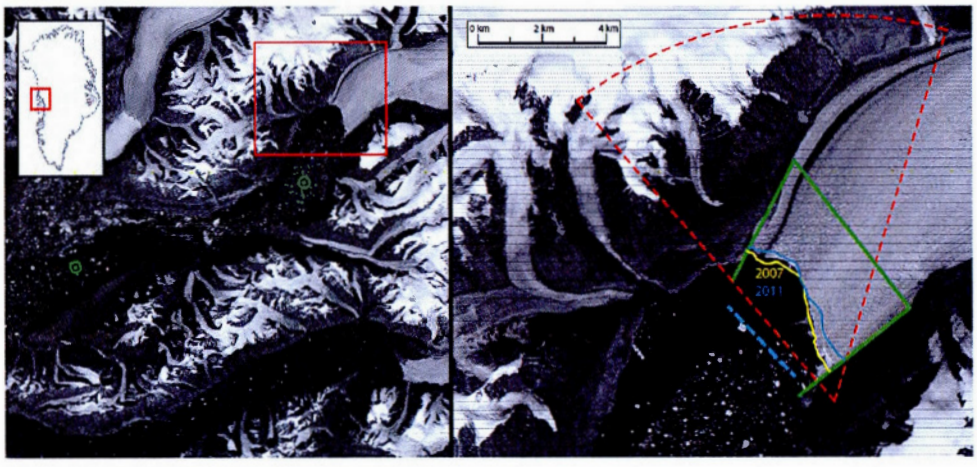

Figure 2.1 Study site. Left: Landsat 7 image (8 July 2014) of Rink Fjord on the west coast of Greenland. Green dots indicate the position at which sea surface temperature (SST) data was extracted around an 8 km radius, 10 (71°39.624N, 51°47.532W) and 40 (71°33.75'N, 52°54.048'W) km from the ice margin. Right: Rink Isbræ calving front with approximate viewshed of the camera marked by dashed red lines. Digitised ice front positions are shown for 2007 (yellow) and 2011(blue). The green reference box was used to calculate area changes between successive Landsat scenes. The dashed blue line about 2 km down the fjord from the ice margin indicates the position of a 200 m high transverse submarine moraine ridge.

2.4 Datasets and Methods

2.4.1 Timelapse cameras

A 10.2 M pixel digital single-lens reflex (SLR) camera (Nikon D200) with a fixed focal length lens (Nikkor 20 mm) was installed on the southern side of Rink Fjord (71°42.348'N, 51°38.055'W) overlooking the calving front (Figure 2.1). The installation was performed by Dr. Jason Box (Geological Survey of Denmark and Greenland, GEUS) for the Extreme Ice Survey (EIS). A custom timer developed

by the US National Geographic Society's Remote Imaging Laboratory was programmed to take daily photographs at 15:00 UTC between June 2007 and July 2011. The camera was enclosed in a Pelican case with a customs-installed optically neutral plastic window, and powered with a 50 Ah gel cell battery connected to a 10 W solar panel. The lack of solar illumination during the polar night and camera malfunction in cold temperatures resulted in data gaps of several months during winter. Additional data loss caused by clouds, fog, and rain drops obstructing the view of the terminus accounts for a loss rate of ~10% for all years of the study period (Table 2.1). In total 803 images were analysed for the entire study period.

Year	Data period	Days	Yearly image loss due to:		Images
			clouds (%)	other (%)	analysed
2007	06.12-10.21	132	10.6	0	118
2008	02.15-10.06	235	10.6	0	210
2009	03.03-08.08	159	10.8	0.7	141
2010	03.31-11.20	236	10.0	3.4	205
2011	01.28-07.21	182	11.0	19.8	129
Total		**944**			**803**

Tableau 2.1 Dataset, study periods and yearly image losses The high percentage of 'other' losses for 2011 are due to the fact that the camera remained operational during the winter (January-February) when cold temperatures (<-30°C) caused temporary sticking of the shutter.

2.4.2 Ice front mapping

Calving front positions were mapped from Landsat 7 Enhanced Thematic mapper Plus (ETM+) band 8 panchromatic images with 15 m pixel resolution. Failure of the scan-line corrector (SLC) on the ETM+ and the resulting offset between scan-lines causes increasing data loss toward the scene edge where banding can reach a maximum width of approximately 400 m. About 15% of scenes were rejected due to significant portions of the front being lost. Useable cloud-free scenes provide data coverage of 3 images per month on average during periods of solar illumination (April-September) for a total of 12-20 images per year. Changes in ice front position between successive images were mapped following the method

described by Moon and Joughin (2008). Retreat and advance was measured using a polygon, bounded on the downglacier side by the ice front which was manually digitised and adjusted to fit the new front position on each successive image, and three fixed lines: two on the sides approximating the lateral margins of the glacier, and one arbitrary line upglacier from the minimum observed front position (green box in Figure 2.1). The average advance or retreat of the front was obtained by dividing the difference in area of two polygons by the mean glacier width. This method accounts for uneven front position variations along the glacier width and allows for a better approximation of advance and retreat as a linear distance.

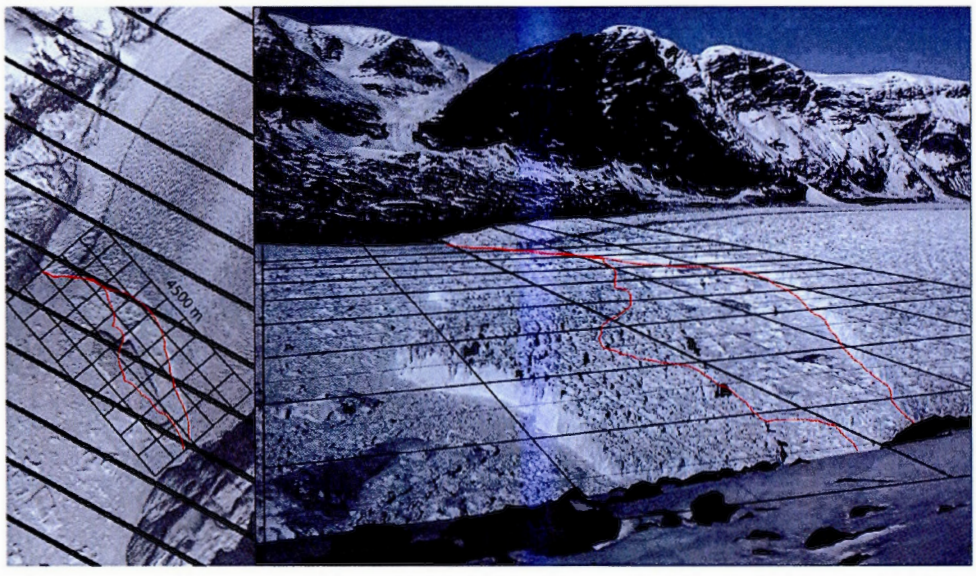

Figure 2.2 Left: Landsat 7 scene from 23 April 2010 with 500 x 500 m grid and digitised position of calving front. Right: Image taken on the same day (15:00 UTC) with approximate grid built based on the Landsat grid. The two red lines indicate the front position before (22 April) and after (23 April) a magnitude 7 event. The size of the calved iceberg is estimated to 1.3 km^2

2.4.3 Calving event magnitude scale

A total of 984 single calving events were documented following a semi-qualitative approach where the size and location of each event was determined using an approximate grid overlaid over the terminus. The 500 x 500 m cells were built by comparing the location of easily identifiable features on select timelapse images

and the corresponding Landsat scenes acquired on the same day (Figure 2.2). The position of the calving front was manually digitised for each daily image and the resulting sequence of vectors was analysed to identify variations in front geometry. Calving event sizes vary from small debris avalanches and isolated blocks detaching from the front, to large events involving nearly the full terminus width. Events were classified following a non-linear magnitude scale ranging from 1 to 7 depending on their relative size. The magnitude was attributed subjectively for each event based on visual observation. The relative size of each event and the associated mass loss were approximated based on the number of 500 x 500 m cells implicated in the event.

Two distinct categories of events emerge from the data. The first consists of magnitude 2-7 events which are large enough to result in an effective retreat of a section of the front (i.e. the new front position is more retracted than the previous one). The second category is made up of magnitude 1 events which consist of debris avalanches and isolated blocks which alter ice front geometry but do not result in retreat. Due to the resolution of the images and the effects of perspective, the method used can introduce a bias when it comes to comparing the relative magnitude of events occurring close to the camera, compared to those happening on the other side of the fjord, 5 km from the camera. Small magnitude 1 events are especially difficult to identify at greater distance and under changing light conditions due to different levels of cloud cover. The presence of ice mélange in the fjord makes it difficult to identify the ice cliffs during winter/spring months, or to pinpoint with precision the day an event occurs. Additionally, the dataset for 2010-2011 was acquired by a different camera located about 100 m away from the first location. The view from the camera therefore changed for the last two years and the first 250 m or so of the front were obscured by rocks. Consequently, the 2010-2011 dataset is missing some of the small events occurring close to the southern margin.

2.4.4 Surface air temperatures and Sea surface temperatures

Sea surface temperatures (SSTs) were obtained from the Moderate Resolution Imaging Spectroradiometer (MODIS) instrument on the NASA Terra satellite.

Daily SST data series were extracted from the MOD28 product with 4.88 km spatial resolution within an 8 km radius of two locations, 10 and 40 km down the fjord from the ice margin (Figure 2.1). The presence of sea ice and ice mélange cover influences temperature derivations and SST data is unavailable during the winter months (January-March). Monthly mean surface air temperatures (SATs) were extracted from measurements acquired every 12 hours by the Danish Meteorological Institute (DMI) at the Qaarsut Airport weather station (70°44'N, 52°42'W; 88 m a.s.l.), located in Uummannaq Fjord, 120 km south of Rink's terminus (Cappelen, 2014). The number of positive degree-days (PDDs) was used as a proxy for surface melt, and to determine the intensity and duration of the melt season. Following the method used by Schild and Hamilton (2013), the onset and the end of the melt season were taken as the first period of five consecutive days where average temperatures were above, or below 0°C.

2.5 Results

2.5.1 Front position change

The width averaged terminus position change calculated from Landsat imagery (Figure 2.3) shows a seasonal variation with an average difference between the annual maximum and minimum position of 670 m, corresponding to 3 km^2 across the whole glacier front. The front typically reaches its seasonal maximum position some time in June and the retreat lasts until the end of September and possibly later, although the precise duration of the retreat phase is uncertain due to the lack of visual data (both Landsat and terrestrial imagery) in late fall and winter. Interannual data shows a relatively stable terminus position with a slight retreat of the seasonal maximum position of $\sim$ 750 m (corresponding to a retreat of 0.8 km^2 a^{-1}) recorded over the study period. The amplitude of seasonal advance/retreat also decreases by over half (from 950 to 360 m) between 2007 and 2011 (Table 2.2).

Year	Maximum position (day of year)	Minimum position (day of year)	Retreat phase (N days)	Area loss (km^2)	Retreat (m)
2007	162	257	95	4.21	950
2008	126	210	84	3.11	660
2009	181	270	89	3.32	730
2010	167	259	92	2.58	590
2011	190	269	79	1.65	360
Average	**165**	**253**	**88**	**2.97**	**658**

Tableau 2.2 Seasonal terminus position variations at Rink Isbræ.

2.5.2 Air and sea temperature

Monthly mean air temperatures measured at Qaarsut over the study period are highest in July (10°C) and lowest in March (-13.9°C). July temperatures show a slight increase of 0.34°C a^{-1} over the study period. The melt season generally lasts from early May until late September with an average duration of 129 days. With the exception of 2010, the year with the longest melt season, where positive temperatures persist for 168 days until late October.

SST data is unavailable for the winter months (January-March) due to sea ice cover. Although sea ice cover remains in the fjord until June, some open water appears in the fjord starting in mid-April. As a result, SSTs increase rapidly in April, reaching a peak in July-August, and decrease more gradually until December. Monthly mean SSTs are consistently higher in the outer fjord location, 40 km from the terminus, with the warmest months showing average temperatures of 1.79°C, compared to -0.57°C in the inner fjord, 10 km away. Additionally, temperatures are more stable in the outer fjord location, possibly due in part to the combined effects of icebergs, brash ice and glacial meltwater mixing closer to the terminus. In the summer of 2010, the warmest year with the longest melt season, average SSTs for the inner fjord location are unusually low, possibly suggesting an increased meltwater discharge. Overall, maximum summer SSTs show a slight increase of 0.26°C a^{-1} over the study period, or 0.59°C a^{-1} when considering only the outer fjord location.

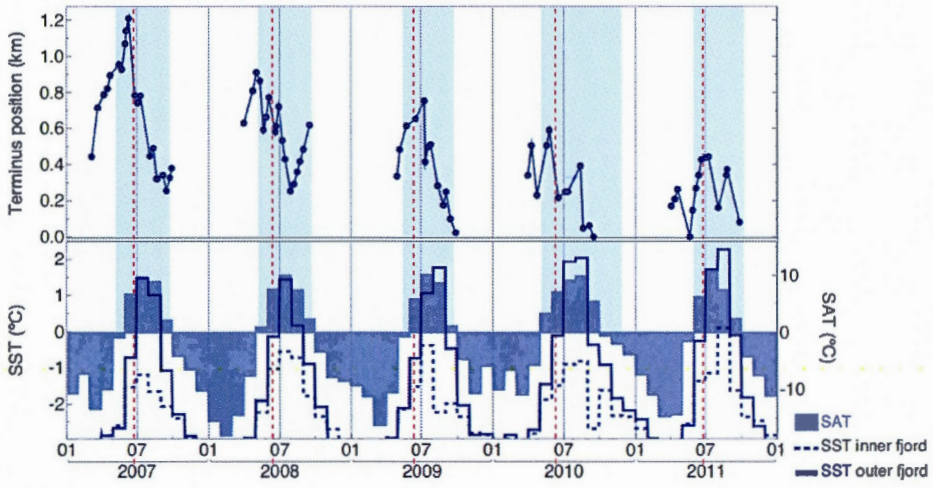

Figure 2.3 Top: Landsat-derived width-averaged terminus position change. Bottom: Monthly mean surface air temperatures (SATs: purple area) and sea surface temperatures (SSTs) for the inner (dashed line) and outer (solid line) fjord locations. The shaded blue area represents the duration of the melt season as derived from positive degree days (PDDs). The vertical red dashed lines indicate the ice mélange clearing day observed on the timelapse images.

2.5.3 Ice mélange clearing date

In winter, sea ice bonds calved glacier ice in the fjord to produce an ice mélange which is pushed down the fjord as the terminus advances. The mélange has been observed to act like a transient thin ice tongue which can generate a small resistive force that stabilises the front and limits calving (Sohn *et al.*, 1998; Joughin *et al.*, 2008c; Amundson *et al.*, 2010; Howat *et al.*, 2010; Nick *et al.*, 2013). Timelapse imagery shows the ice mélange to form progressively starting in January or February, and to stiffen throughout the winter to reach maximal thickness in March or April. 2011 is the only year with visual data covering the initial formation of the mélange. That year, the fjord remains free of ice until mid-February and the mélange only reaches maximum integrity in mid-May. In April it is thin enough that large cracks, a few kilometres long, break the sea ice revealing some open water. The fjord remains choked up until late June (day 176), about 3 weeks later than the previous year. The day of mélange clearing (or mélange breakup) at the terminus can be precisely identified on the terrestrial imagery which shows a rapid

disintegration occurring over the span of one to a few days. The day of clearing is taken as the first day on which icebergs move independently from each other. There appears to be no clear relationship between the start of the melt season and the day of mélange clearing. There is however a correlation between mélange breakup and May SSTs, which is consistent with the observations of Howat *et al.* (2010). The earliest day of clearing is recorded at the beginning of June in 2010 (day 152) following a particularly mild winter and the highest May SSTs in the study period. Both 2007 and 2011 experience late mélange clearing dates near the end of June(days 175 and 176 respectively) as well as low May SSTs.

Year	Start (day of year)	End (day of year)	Duration (N days)	Ice mélange clearing (day of year)
2007	131	264	133	175
2008	131	263	132	165
2009	137	262	125	163
2010	128	296	168	152
2011	153	277	124	176
Average	**136**	**272**	**136**	**166**

Tableau 2.3 Melt season duration and ice mélange clearing date from Rink Fjord.

There appears to be no strong relation between the timing of the terminus maximum position and that of the mélange clearing in Rink Fjord (Figure 2.3). As retreat is intimately linked to calving rates, if a major event occurs shortly before the mélange breaks up, the front position recorded immediately preceding that event will be documented as the yearly maximum position. This appears to be the case for 2007 and 2008 where magnitude 7 events occurred 10 and 4 days before mélange breakup respectively. On all other years advance continued and the maximum position was reached after the mélange cleared the fjord.

2.5.4 Event size distribution

Calving event sizes show a highly skewed distribution with a mean magnitude between 1 and 2 on a 1-7 scale (Figure 2.4). Of the 984 events documented, 73% are categorised as magnitude 1 and consist of isolated blocks or small debris avalanches. The largest magnitude 7 events represent only 1% of all calving activity, and produce massive tabular icebergs over 1 km^2 surface area. Although

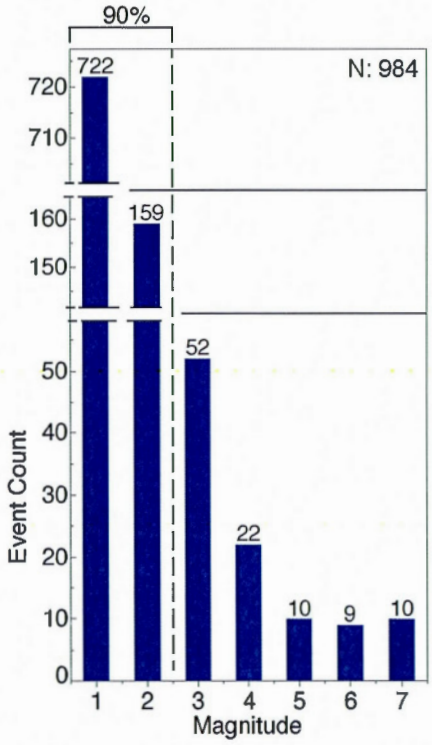

Magnitude	Of all events	Mass loss
	%	%
1	73	–
2	16	8
3	5.3	11
4	2.2	11
5	1	10
6	0.9	16
7	1	44

Figure 2.4 Left: Event size distribution. Magnitude 1 and 2 events represent nearly 90% of all events while large magnitude 5, 6 and 7 events account for ~1% each. Right: Estimated relative contribution to mass loss for each magnitude. The mass loss estimates do not take into account the magnitude 1 events due to the large uncertainty involved in estimating their relative size.

infrequent, the magnitude 7 events contribute 44% of all mass loss compared to only 8% for those of magnitude 2.

Figures 2.5, 2.6, and 2.7 present the temporal distribution of all events over the entire study period. Events of magnitude 5, 6, and 7, here considered to be major events, occur between 3 and 9 times per year with inter-event intervals ranging from a few days to as long as 2 months for an average of 38 days. Smaller events experience significantly shorter repeat intervals, with multiple events occasionally occurring on the same day. Events of magnitude 1, 2, and to some extent, 3, all experience a marked increase in frequency in June immediately after the day of mélange clearing, reaching a clear peak in July. For two of the five years (2007

and 2008), the frequency of small events decreases in August-September. Data covering the end of the summer period are not available for 2009 and 2011, and 2010 presents generally low calving activity and a slowdown is not observable. Major events appear to lack such seasonality, suggesting that they are driven by different processes. Interannual variability in event size distribution is not available for all months due to uneven coverage provided by the dataset. However, some comparison is possible for 6 months, between April and September. Both 2010 and 2011 appear to exhibit subdued calving activity when it comes to small (magnitude 1 and 2) events. This can at least partly be explained by the change of camera position which ended up hiding most activity occurring at the first 200-250 m of the front from 2010 onwards. In the first three years, ~30% of the observed magnitude 1 events occurred within the first 250 m. This number drops to ~7% for the last two years. This observational bias creates no significant difference in the occurrence of larger events of magnitude 2 and higher.

2.5.5 Calving styles and calving front geometry

Most days experience one or occasionally two events, not considering the isolated blocks detaching from the front (i.e. magnitude 1 events). One major drawback of the method used is that the sampling rate does not allow to determine whether the mass lost in the 24 h period between images is the result of one major event or of multiple smaller ones. It would therefore be useful to increase the sampling rate and acquire for example hourly photographs during periods of high calving activity. This explains in part the negative relationship between major events and smaller ones, which is the fact that fewer small events are detected on days where larger sections of the front collapse, because the large events wipe the little ones from the record. Major events affect the full thickness of the terminus, extend over several kilometres (up to 4 km) across the front and produce an ice margin with a regular, linear or arcuate, geometry. Small events on the other hand cause the ice cliffs to become irregular and punctuated by small embayments.

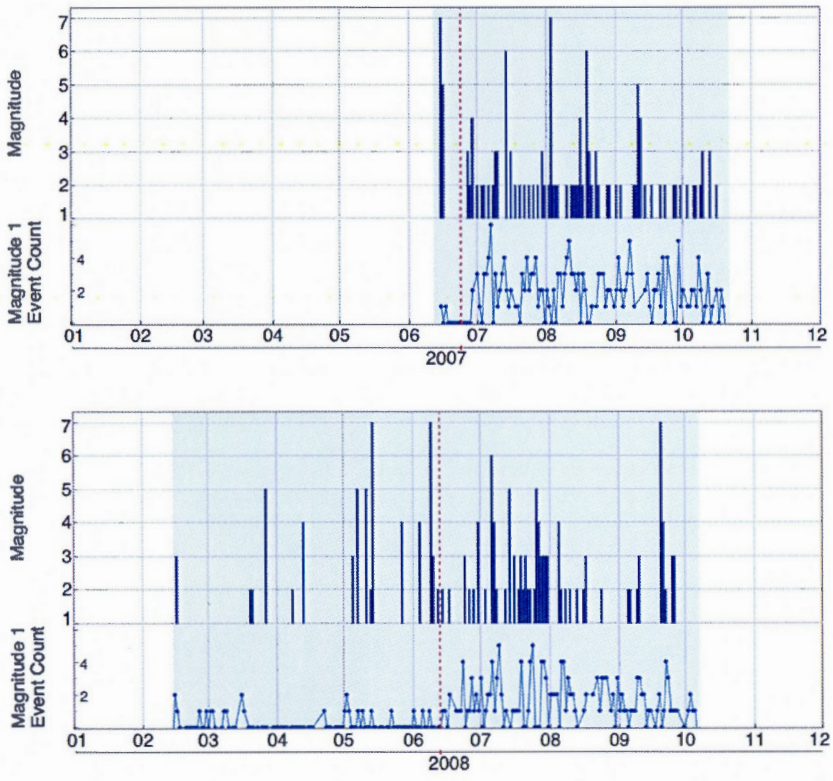

Figure 2.5 Magnitude of daily calving losses for 2007 and 2008. The red dotted line represents the day of mélange clearing. Events of magnitude 1 are represented separately as they tend to have a much higher frequency with as many as 6 events occurring per day. On days where 2 larger events occur, their magnitudes are joined in one single value. As this is a non-linear scale, two distinct magnitude 2 events are not necessarily equivalent to a magnitude 4 event. The grey shaded area indicates the time periods for which data are available.

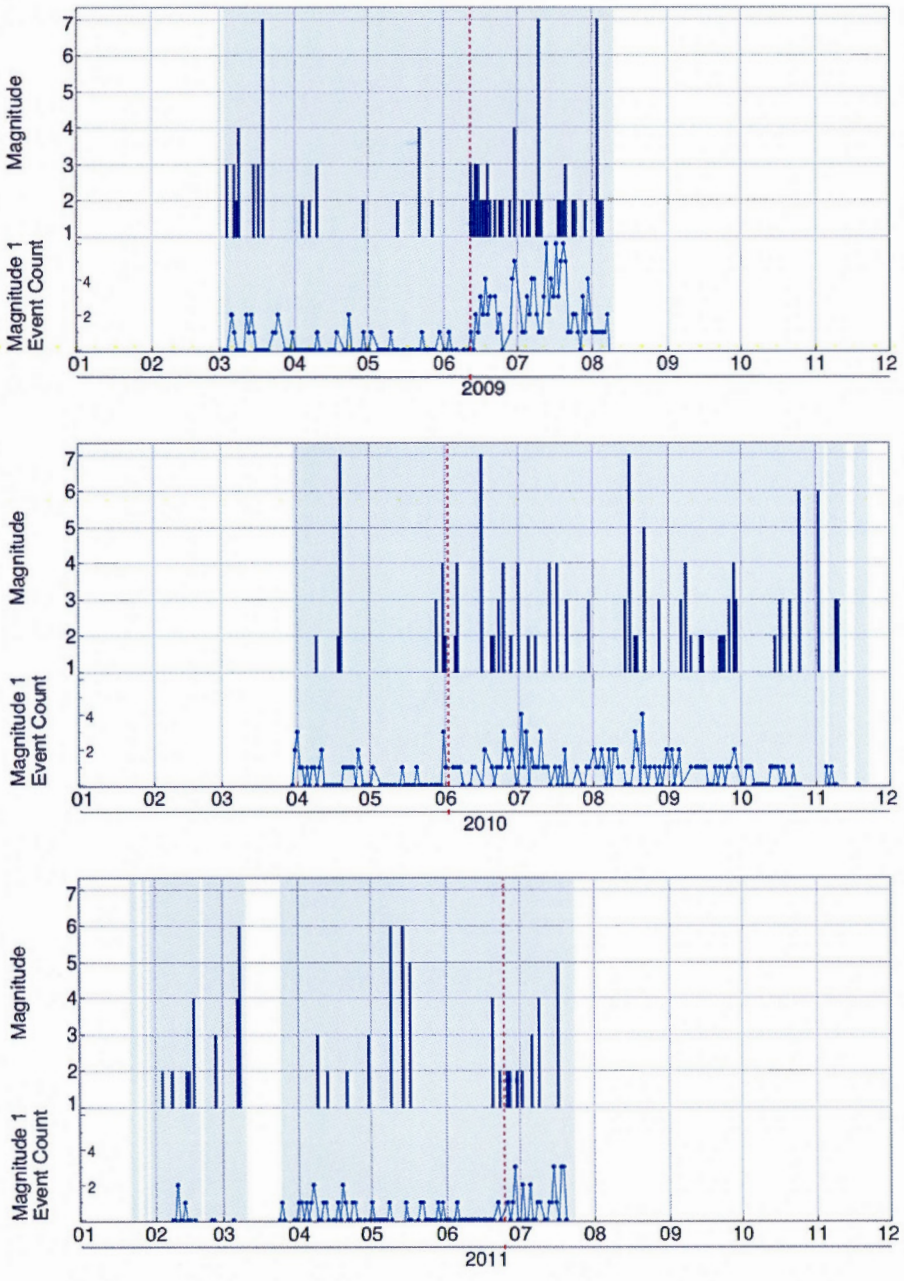

Figure 2.6 Magnitude of daily calving losses for 2009, 2010, and 2011 (same as previous figure)

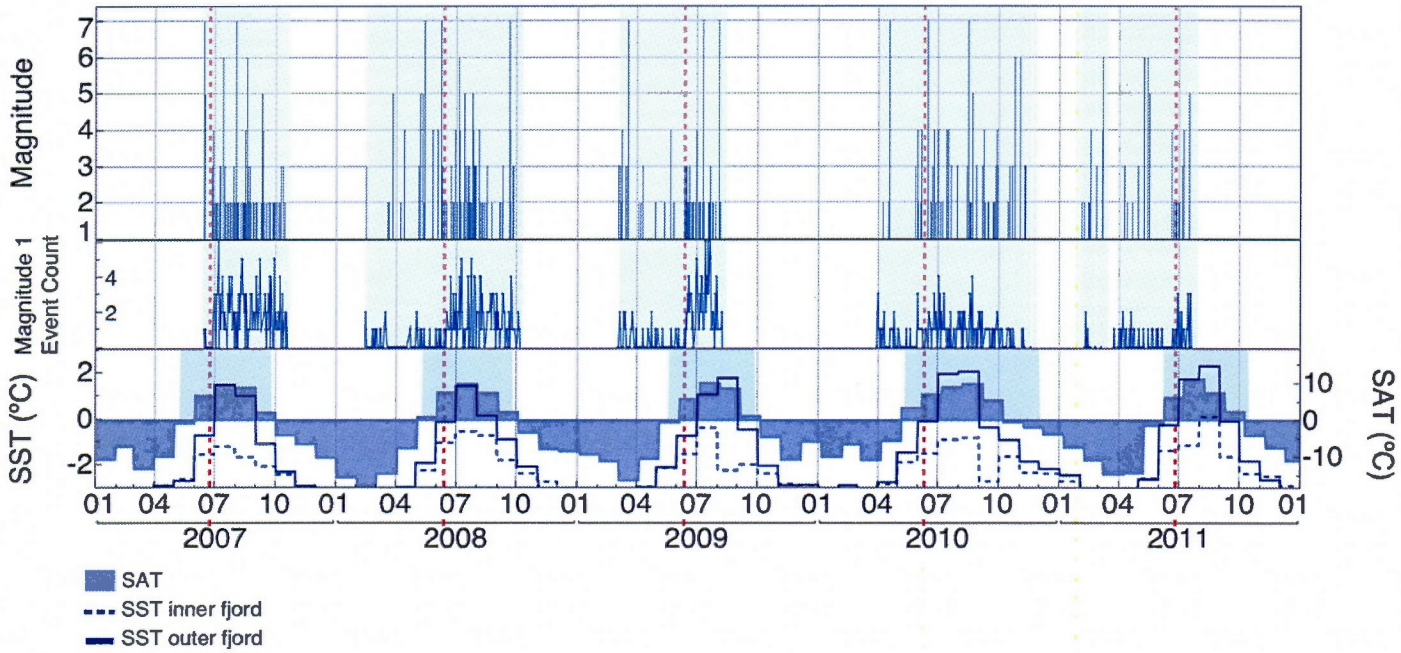

Figure 2.7 Top: Magnitude of daily calving losses for all years. Bottom: Monthly mean SATs (purple area) and SSTs for the inner (dashed line) and outer (solid line) fjord locations. The shaded blue area represents the duration of the melt season as derived from PDDs. The vertical red dashed lines indicate the ice mélange clearing day observed on the timelapse images.

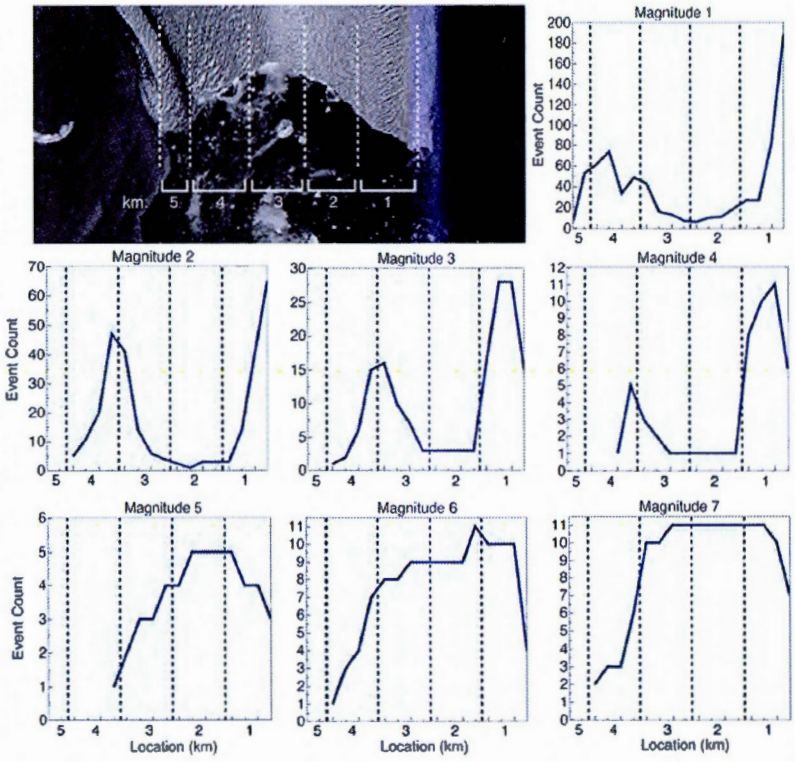

Figure 2.8 Spatial distribution of all logged calving events across the 4.5 km-wide front divided into 18 sections of 250 m each. Notice the different scale for the vertical axis showing event count. The north side of the fjord is on the left.

The spatial variability of calving across the front was analysed by dividing the front into 18 sections of approximately 250 m each and documenting the location of each event (Figure 2.8). Magnitude 1-4 events exhibit a strong bimodal distribution with two peaks, one located at kilometre 1, and the other at the limit between kilometre 3 and 4. The significantly stronger peak on the southern side of the fjord likely represents a bias introduced by the perspective of the images and the difficulties in identifying events further away from the camera. Major events of magnitudes 5-7 on the other hand affect larger portions of the front and often extend over multiple kilometres (up to 4 km) across the front. Their distribution is therefore wider, with a shift towards the southern side of the fjord. Landsat imagery (Figure 2.9) shows that they clearly align with the least crevassed sector of the terminus which also corresponds to the area with the deepest water and

highest ice velocities (Chauché *et al.*, 2014). As the major events appear to be responsible for most of the mass loss through calving, the central sector of the front experiences significantly higher losses than the margins. The spatial distribution of low magnitude calving events on the other hand coincides with areas closer to the margins, with closely spaced crevasses which experience a higher frequency of events.

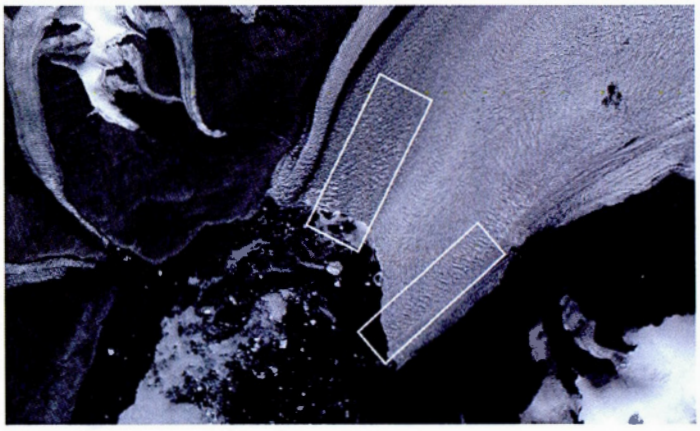

Figure 2.9 Landsat image (20 June 2014) showing the pattern of surface crevasses. The white rectangles indicate de two highly crevassed sectors of the terminus.

Figure 2.10 Calving front geometry before (06 May 2009) and after (16 June 2009) mélange clearing. Embayments form in locations where calving picks up rapidly following mélange breakup.

The rapid increase in calving rates occurring at the time of ice mélange clearing mainly concerns the low magnitude events and affects the more crevassed areas of the front. On four of the five years, large embayments are observed to form

rapidly over a few weeks in June as the mélange disintegrates. The mélange first loses its integrity near the lateral margins and calving rapidly picks up at these locations resulting in retreat. At the same time, the middle section of the front continues to advance forming a large headland which extends as far as ~1 km further out into the fjord (Figure 2.10). The advance of the headland is rather short-lived and it quickly disintegrates in a series of larger events returning the front to a more linear geometry in a matter of weeks.

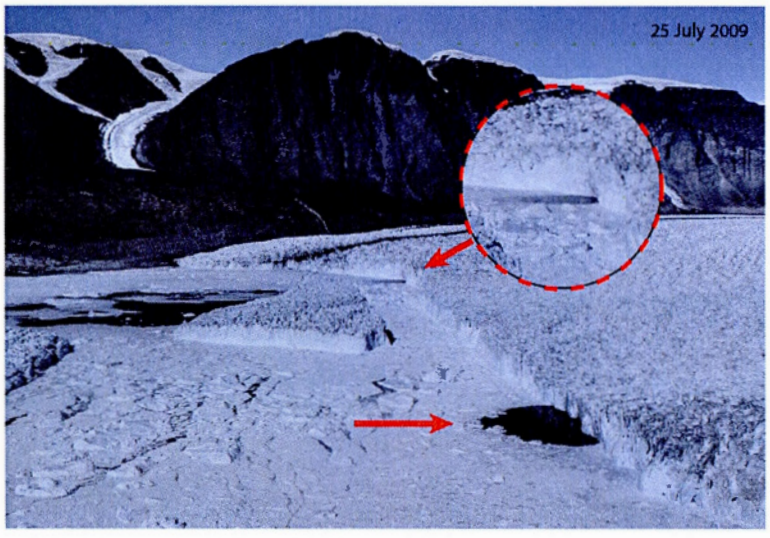

Figure 2.11 Typical locations of glacial meltwater upwellings.

The spatial distribution of small events additionally seems to correlate with the spatial pattern of upwellings of glacial meltwater. Upwellings are observed on the timelapse imagery between June and September as well-defined plumes pushing brash ice away from the ice cliffs (Figure 2.11). Localised meltwater discharge at the front has been observed to increase submarine melt rates which leads to undercutting of the ice cliffs and modifies the force balance at the front by removing supporting ice (Motyka *et al.*, 2003; O'Leary and Christoffersen, 2013; Chauché *et al.*, 2014). Locations where meltwater emerges at the front are therefore expected to experience increased calving rates which creates a characteristic front geometry punctuated by embayments. At Rink those embayments remain small and rather short-lived and the front remains relatively linear throughout the summer.

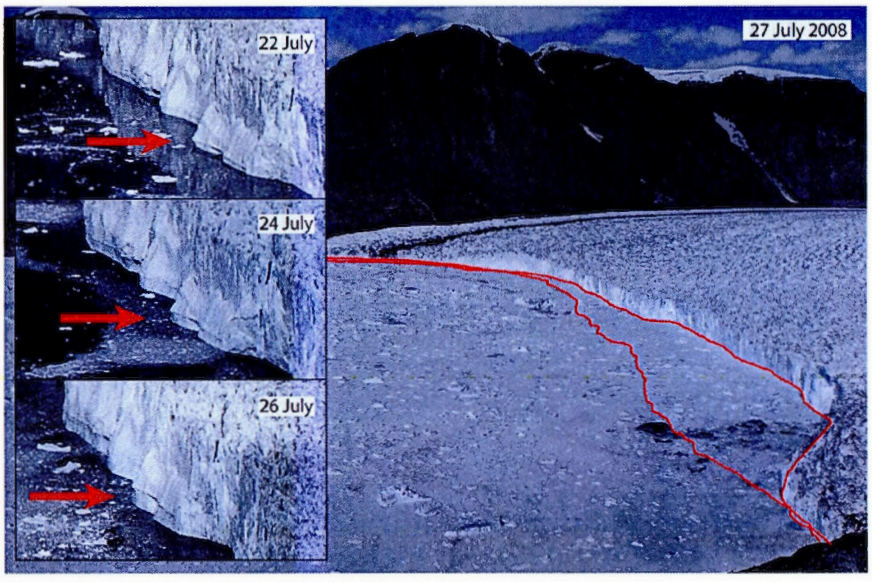

Figure 2.12 A notch appears above the waterline on 19 July and is raised increasingly higher until a magnitude 5 event on 27 July leads to a ~100 m (width-averaged) retreat of the front.

By removing ice at and below the waterline, submarine melt can additionally lead to the development of a notch (O'Leary and Christoffersen, 2013). This process has been identified at a number of lake-terminating glaciers (Kirkbride and Warren, 1997; Benn *et al.*, 2001; Röhl, 2006), and one tidewater glacier on Svalbard (Vieli *et al.*, 2002) as having a direct control on calving rates. At Rink, undercutting produces a notch at the waterline which promotes a bottom-up calving style in which flakes breaks off just above the waterline leaving the higher portion of the cliff unsupported. Detachment of the ice above the overhang usually follows within a few days. On several occasions the notch is observed to grow as it is raised progressively higher above the waterline. The lifting front is here taken as evidence of backward rotation of the terminus (Benn *et al.*, 2007b) affecting the middle, less crevassed sector of the front. Back-tilting of the front was observed immediately preceding a few major calving events resulting in the detachment of large tabular icebergs. For example, in July 2008, the front was observed to rotate over a period of a week, accelerating progressively until failure occurred about 300 m further upglacier resulting in a magnitude 5 calving event (Figure 2.12). This

process occurs at least twice a year, in July and August, and always precedes the detachment of large icebergs. Back-tilting of the terminus is however not observed before every major event, even during the melt season when the notch is visible but remains relatively low at the waterline. In periods of the year when melt at the waterline is low, back-tilting may still occur without providing any easily identifiable visual evidence.

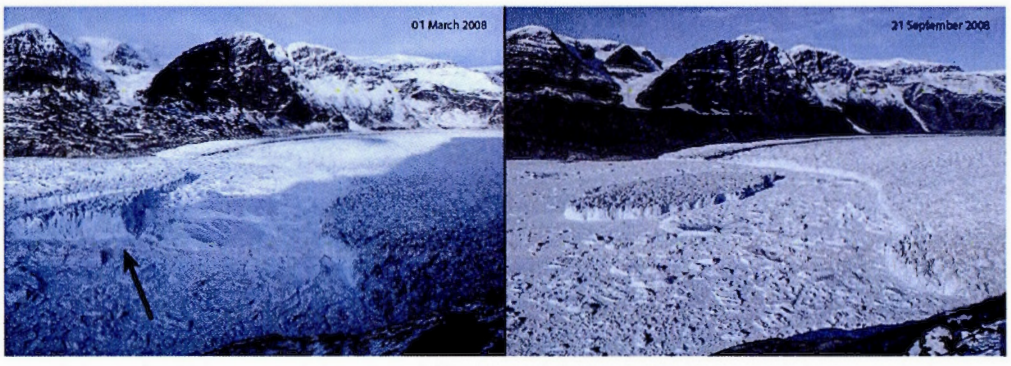

Figure 2.13 Left: Ice mélange on 01 March 2008 with both overturned and tabular icebergs bonded together by sea ice. The berg marked with the arrow is no more than 500 m wide in the glacier flow direction. Without the stabilising effect of the sea ice it would have most likely capsized. Right: Magnitude 7 calving event on 21 September 2008 with tabular iceberg (~2000 x 800 m) and fjord filled with brash ice and overturned berg fragments.

Most of the observed calving events produce icebergs which break into a few large blocks and rotate onto their sides, or disintegrate completely filling the fjord with brash ice. Of the major events only about a third produce full-thickness tabular icebergs which remain relatively intact following detachment. With the exception of a few events occurring in the winter when the sea ice stabilises calved ice, all the tabular bergs are 1-4 km long and over 650 m wide (in the glacier flow direction). More commonly, icebergs are narrower, with a width smaller than the ice thickness. This specific aspect ratio causes them to overturn due to buoyant forces, unless ice mélange is present to provide a sufficiently important resistive force (Amundson *et al.*, 2010) (Figure 2.13). Occasionally the tabular bergs remain pinned between 1 and 2 km from the front as they probably become grounded on the submarine ridge extending across the fjord.

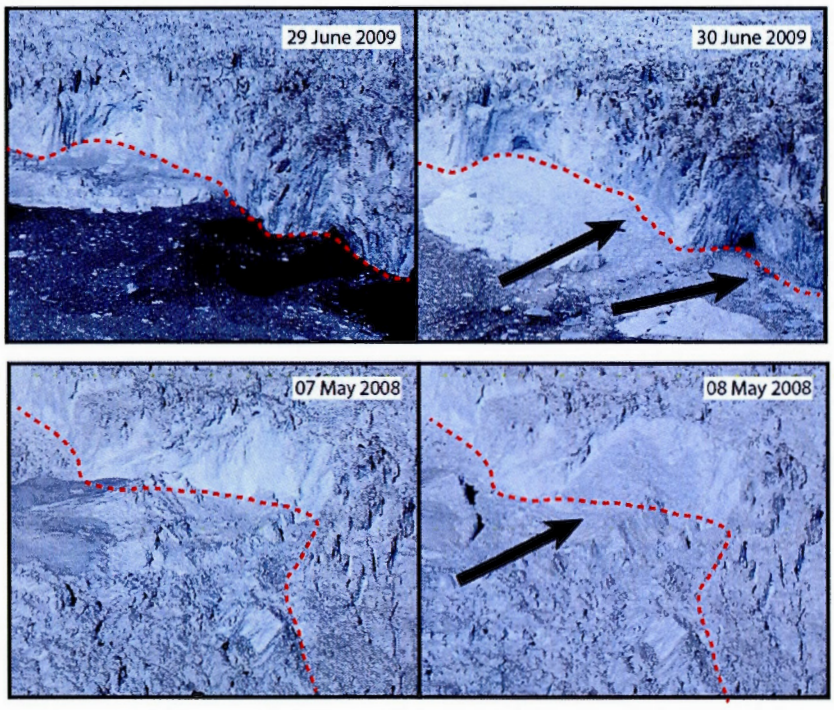

Figure 2.14 Top: Summer calving with magnitude 1 events consisting of distinct blocks detaching from the front. Smaller events often occur in close proximity to portals where meltwater is injected into the fjord. Bottom: Winter calving with debris avalanches and a slumping ice margin. The position of the front is difficult to distinguish from the ice mélange as they tend to form a continuous mass.

Occasionally, rifts, or large transverse crevasses opening across the terminus, are observed one or a few days before a major calving event. Due to the delay between rift formation and iceberg detachment it is at times difficult to identify the day on which the event occurs. This is particularly the case in the winter where the ice mélange transfers enough backstress to the glacier front to prevent the berg from floating away immediately upon rift formation (Amundson *et al.*, 2010). Winter front geometry is characterised by sloping ice cliffs and magnitude 1 events often consist of debris avalanches and block slumps which accumulate at the base of the cliffs. As winter progresses rifts fill up with snow and the ice cliffs, ice debris, and mélange grow to form a single mass with no discernible glacier front.

2.6 Discussion

The timelapse imagery recovered at Rink provides evidence of two different calving styles with distinct temporal and spatial distributions. This suggests that calving is driven by two distinct (sets of) mechanisms, each having a specific effect on terminus geometry. Small events show a marked increase in frequency immediately following ice mélange breakup and tend to occur preferentially at highly crevassed areas. These areas coincide with locations where buoyant meltwater emerges at the terminus, suggesting an influence of melt-driven processes. Major events on the other hand display little seasonal variability and occur at irregular intervals throughout the year. They mostly affect the central, less crevassed section of the front with the highest ice velocities and greatest water depth. The raised waterline notches provide evidence of back-tilting of the terminus, which suggests that major events are mechanically-driven and occur in response to buoyant flexure. The different observed calving patterns may therefore also be related to the variability of buoyancy conditions at the terminus.

2.6.1 Melt-driven calving

Submarine melt has a major impact on terminus stability and on some glaciers estimates of submarine melt rates are significantly larger than surface melt rates (Motyka *et al.*, 2003, 2011; Rignot *et al.*, 2010; Jenkins, 2011; Enderlin and Howat, 2013). At Rink, Enderlin and Howat (2013) estimated mean submarine melt rates of 2.42 m d^{-1} (with an uncertainty of 3.26 m d^{-1}), while surface melt rates are averaged at a mere 0.0009 m d^{-1} for the 2000-2010 period. Rignot *et al.* (2010) measured submarine melt rates at west Greenland glaciers and estimated that approximately half of the mass loss at the front was directly due to melt and the rest through the calving of icebergs. However, frontal melting is not only important as a mass balance term and has been shown to affect calving processes by modifying front geometry. O'Leary and Christoffersen (2013) modelled the effects of submarine melt on the stress patterns at the ice front and found that undercutting of the ice cliffs directly leads to increased calving rates, with larger events occurring with higher melt rates. The sensitivity to undercutting may be heightened when melt is concentrated at the waterline resulting in the formation

of a notch which leaves a portion of the ice cliffs unsupported and more prone to calving (Cook *et al.*, 2014).

Submarine melt is influenced by both water temperatures and fjord circulation patterns. There appears to be no direct relationship between MODIS SSTs and calving rates, indicating that surface water temperature is not the primary control on submarine melt and undercutting. It is however likely that water temperatures at the base of the glacier have a greater impact on calving processes than those measured on the surface (O'Leary and Christoffersen, 2013). Chauché *et al.* (2014) reported the presence of warm (2.8 ± 0.2°C) Atlantic water below 400-500 m depth in Rink Fjord. With an ice depth of ~750 m, an extensive section of the glacier front is exposed to this warm water mass which significantly influences submarine melt at depth. A number of studies have additionally recognised the crucial role of cold freshwater discharge in enhancing submarine melt rates. Buoyant freshwater plumes play a crucial role in fjord circulation patterns as they drive forced convection and the entrainment of warm water to the ice front (Motyka *et al.*, 2003; Rignot *et al.*, 2010; Jenkins, 2011; Straneo *et al.*, 2011; Xu *et al.*, 2012; Sciascia *et al.*, 2013). At Rink, upwellings of meltwater are repeatedly observed on the timelapse imagery throughout the summer (Figure 2.11). Chauché *et al.* (2014) additionally identified turbid waters below the surface indicating that freshwater and turbulent mixing is present at depth even when evidence at the surface is lacking. Analysis of the spatial calving patterns indicates that low magnitude events are mainly concentrated near conduits where undercutting rates are expected to be at their highest. Calving rates peak in July, coinciding with the highest air temperatures and enhanced meltwater production, and decrease at the end of the summer as temperatures and runoff drop.

It is noteworthy that the same spatial pattern also characterises winter calving, when submarine melt rates are at their lowest, which indicates that undercutting is not the only mechanism driving calving. The spatial distribution of low magnitude events also coincides with highly crevassed areas of the terminus. It is therefore suggested that preexisting crevasses advected from regions of high tensile stresses further upglacier provide points of weakness along which iceberg detachment is more likely to occur. Although a highly fractured terminus is more prone to

calving, additional forces may be necessary to break the equilibrium and trigger calving events (Bassis and Jacobs, 2013). In this perspective, undercutting may be considered as an additional perturbation promoting the detachment of bergs from an already fractured front. The input of meltwater into surface crevasses has also been proposed to act as an enhancing factor as it can lead to hydrofracturing. This can cause fractures to deepen and potentially propagate through the full thickness of the glacier and lead to calving (van der Veen, 1998, 2007; Vieli and Nick, 2011; Cook *et al.*, 2012). Together with undercutting, the presence of more surface meltwater in the summer months could also contribute to the seasonal pattern of low magnitude events. Surface runoff is therefore hypothesised to play a dominant role in driving summer calving rates in the highly fractured areas of the ice margin.

2.6.2 Mechanically-driven calving

Submarine melt and undercutting of the ice front affect both grounded and floating termini as they lead to grounding line retreat as well as thinning of floating sections (Rignot *et al.*, 2010; Straneo *et al.*, 2010; Motyka *et al.*, 2011; Seale *et al.*, 2011; Münchow *et al.*, 2014). O'Leary and Christoffersen (2013) found that submarine melt at the front has the largest effect on calving when the glacier is already near floatation. This is because floating termini are subjected to buoyant forces which impose a torque on the floating ice tongue at the junction between the grounded and buoyant sections of the glacier margin. Further thinning of the terminus causes it to become increasingly out of equilibrium with the hydrostatic pressure and can then lead to the breakup of the floating ice tongue (Benn *et al.*, 2007b; Pfeffer, 2007; Nick *et al.*, 2009).

Thinning can additionally occur as a dynamic adjustment in response to increases in ice velocities and the resulting variations in longitudinal stress gradients (Pfeffer, 2007; Nick *et al.*, 2009). Velocity variations at Rink are correlated with seasonal changes in front position, with increased ice flow occurring during summertime retreat (Howat *et al.*, 2010). The same was also observed at Jakobshavn Isbræ where seasonal acceleration is hypothesised to occur in response to a reduction in backstress brought on by terminus retreat (Joughin *et al.*, 2008a,c).

Using a numerical ice-flow model, Nick *et al.* (2009) showed that outlet glaciers adjust rapidly to changing boundary conditions at the ice margin in response to variations in longitudinal stress gradients. Through the transfer of longitudinal stresses, a perturbation at the terminus such as a reduction in backstress due to calving-driven retreat, may trigger an immediate velocity increase up to 20 km upglacier. Large calving events, or the loss of a portion of a floating ice tongue can therefore substantially modify the longitudinal force balance at the terminus, and lead to acceleration, stretching, and dynamic thinning (Joughin *et al.*, 2004, 2008b; Thomas, 2004; Howat *et al.*, 2005; Nettles *et al.*, 2008; Nick *et al.*, 2009; Vieli and Nick, 2011). The yearly fluctuations in front position (400-1000 m) observed at Rink may also modify stress patterns and explain the $\sim$ 25% seasonal velocity variations. Extensional flow and the associated dynamic thinning are therefore likely to increase buoyancy near the calving front and lead to the calving of large tabular bergs. Smaller surface slope gradients additionally allow a larger area of the front to thin to floatation which increases the area of the terminus affected by buoyancy variations and can promote further retreat (McFadden *et al.*, 2011). Buoyancy conditions at the terminus therefore depend on its geometry, including ice thickness and surface slope, as well as bed topography. At Rink, large tabular icebergs tend to detach in the midsection of the ice margin. Due to deeper water and higher ice velocities, the centre has a greater tendency for extension and floatation, promoting the large full-depth mechanically driven calving events. The contrasting calving patterns affecting the areas near the margins could be partially explained by the variability in buoyancy conditions across the terminus. Grounded areas would tend to experience smaller, and more frequent, calving activity.

The lifting of the notch above the waterline during summer months provides evidence for flexure at the front which occurs when the terminus thins below its floatation thickness. In response to buoyant forces, the floating ice tongue is raised and back-tilted (Benn *et al.*, 2007b). The same mechanism of ice front rotation was observed to lead to major calving events at Helheim Glacier where buoyant flexure caused a large surface depression to form near the grounding line and calving occurred though the propagation of basal crevasses (James *et al.*, 2014). At Rink, detachment of back-tilted portions of the terminus occurs hundreds of

meters behind the terminus but the location of failure varies between events. This suggests that detachment does not necessarily occur near the grounding line so that buoyant flexure only removes sections of the floating ice tongue. Often times, major calving events occur without any signs of back-tilting. This may be because a minimum amount of rotation, too small to be recorded on the timelapse imagery, is sufficient to cause large basal rifts to propagate to the surface and lead to calving. The response of the terminus to variations in buoyancy may essentially depend on how the terminus manages to accommodate the resulting changes in the force balance. The determining factor may therefore be how quickly the terminus approaches floatation, and how quickly it compensates for it. According to theory, progressively increasing upward bending forces can be accommodated by ice creep, but rapid perturbations are more likely to lead to mechanical failure, fracture propagation, and calving (Benn *et al.*, 2007b; Boyce *et al.*, 2007). Another possibility is that rotation is not a prerequisite for calving and that in some cases bergs may breakoff through progressive rift propagation induced by longitudinal stretching. Where neither rifts nor rotation are visible, what appears like one major event might instead be the result of multiple smaller events which are not recorded on the timelapse imagery due to the sampling rate.

The fact that the detachment of large tabular icebergs is sporadic and displays only a weak seasonal signal indicates that the terminus remains close to floatation throughout the year. However, enhanced melt in the summer (both basal and surface), as well as dynamic thinning, has the potential to additionally reduce backstress and modify buoyancy conditions at the terminus. This would explain the seasonal behaviour of winter advance and summer retreat. As the major events are are responsible for most of the mass lost through calving, they must also, together with frontal melt, be accountable for some of the seasonal length fluctuations of the floating ice tongue.

2.6.3 Ice mélange dynamics

Ice mélange dynamics are here discussed separately, yet it should be noted that sea ice conditions in the fjord exert a mechanical forcing on the terminus, and that mélange strength is also influenced by melt. Both oceanic and atmospheric

conditions have a major impact on sea ice concentrations and the integrity of ice mélange, which has been reported as being an important influence on the timing of calving events, as well as a contributor to the seasonal advance and retreat cycle. Several studies have found that the consolidation of ice mélange in winter months suppresses calving by progressively building up backstress (Sohn *et al.*, 1998; Reeh *et al.*, 2001; Joughin *et al.*, 2008c; Amundson *et al.*, 2010; Howat *et al.*, 2010; Murray *et al.*, 2010; Herdes *et al.*, 2012; Walter *et al.*, 2012; Nick *et al.*, 2013).

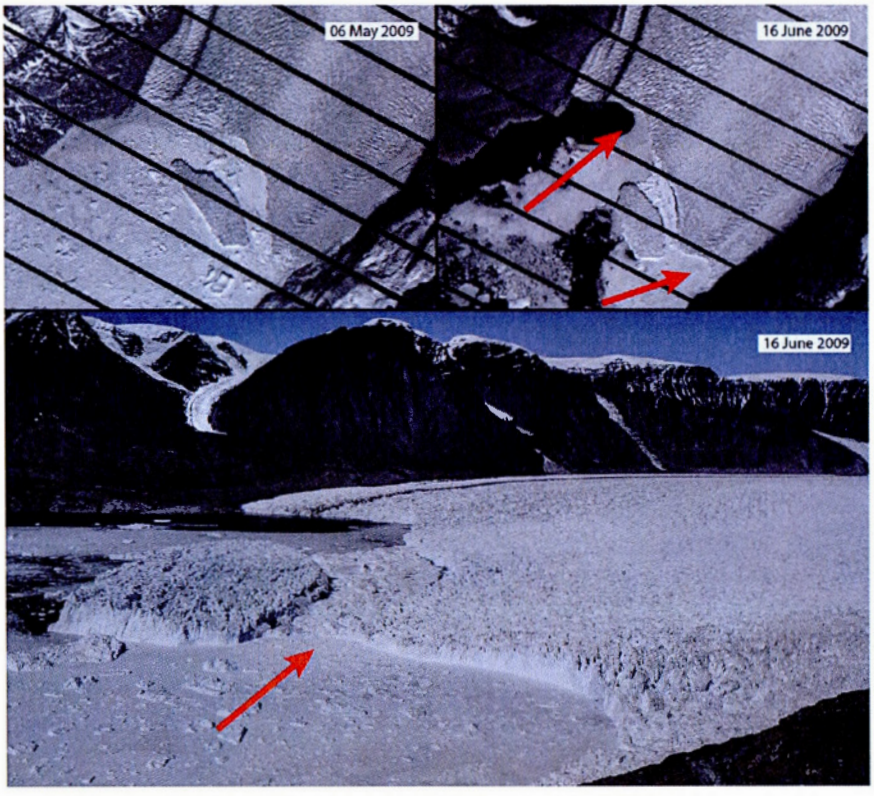

Figure 2.15 Calving pattern after mélange clearing. Top: Calving front geometry before (06 May 2009) and after (16 June 2009) mélange clearing. Embayments form in locations where calving picks up rapidly following mélange breakup near the lateral margins. Bottom: The tabular iceberg stabilises the ice mélange and keeps it pinned to the front of the glacier. This may allow the midsection of the terminus to advance further into the fjord.

In agreement with theory, the frequency of low magnitude events increases rapidly

as the ice mélange weakens in June. In general, the mélange first loses its integrity near the margins, in areas where the terminus is more crevassed and small events dominate, and persists a few days longer in the middle sector of the front. The margins then experience rapid retreat which leads to the formation of two embayments separated by a large headland. In 2009, the headland is observed to advance further out into the fjord than any other year, possibly due to the presence of a large tabular iceberg which appears to remain grounded on the submarine ridge extending across the fjord (Figure 2.15). While pinned down, this berg exerts a compressive force and stabilises the mélange, allowing it to keep its integrity for longer. It may also stabilise the midsection of the glacier front, allowing it to advance further while calving picks up rapidly near the lateral margins. After the tabular iceberg and the rest of the mélange clears the fjord, the headland eventually breaks away in one major calving event. However, in most years, the advance of the headland continues even after the mélange completely clears the fjord suggesting that the midsection of the ice front is less sensitive to ice conditions in the fjord than the more crevassed areas at the margins.

The lack of close relationship between the timing of the maximum frontal position and of ice mélange breakup is most probably due to the episodic occurrence of major calving events. As mentioned earlier, if an event causes a substantial retreat shortly before mélange clearing, the yearly maximum position will be recorded immediately preceding that event. In most years however, the front reaches its most advanced position after mélange breakup as the midsection continues to advance. Although the major calving events are not entirely prevented by the presence of ice mélange in the fjord, calving-related terminus retreat observed in the winter is small compared to the cumulative mass loss recorded in summer. It is therefore possible that the presence of the ice mélange has a stabilising effect on the front allowing it to advance further into the fjord.

Cook *et al.* (2014) modelled the effect of ice mélange on longitudinal stress gradients and found that realistic values of backstress were insufficient to significantly influence the crevasse patterns around the terminus. Although the mélange might be too weak structurally to influence the propagation of fractures, Amundson *et al.* (2010) suggested that is may have a stabilising effect by preventing ice-

bergs from overturning and drifting away from the terminus. This effect is clearly visible in the winter when the mélange effectively stabilises calved ice and partially counteracts buoyancy forces which would otherwise cause most icebergs to capsize. However, the ice mélange is not entirely rigid and some of the icebergs embedded in the sea ice occasionally break off into smaller fragments which then overturn. The energy released by the movement of those blocks contributes to weaken the mélange in the fjord which undermines its stabilising effect on the front (Amundson *et al.*, 2010; Howat *et al.*, 2010). The rapid increase in calving rates in the highly crevassed areas of the front immediately following mélange breakup suggests that the backstress may indeed prevent the already fractured areas of the front from disintegrating and the icebergs from drifting away. The delayed response of the middle sector may be due to its lower sensitivity to variations in backstress which prove to be insufficient to initiate fracture propagation. As with the submarine melt and undercutting, the loss of backstress due to ice mélange breakup in June may represent another mechanism capable of providing additional perturbations leading to the detachment of icebergs from an already fractured front.

Separating the influence of both melt-induced processes (undercutting and hydrofracuring), and ice mélange variations on terminus behaviour is not straightforward. Although mean surface air temperatures indicate that the melt season starts in May, calving rates remain low until the ice mélange clears the fjord, which points to sea ice conditions as a controlling mechanism. However, calving activity peaks in July, coinciding with the highest air temperatures and drops slightly near the end of the summer, suggesting an influence of meltwater runoff. The correlation between May SSTs and the day of mélange clearing indicates that the integrity of the mélange is affected by submarine melt, although other factors such as strong winds may also weaken the mélange (Walter *et al.*, 2010; Christoffersen *et al.*, 2012). Both calving rates and ice mélange strength and extent are therefore influenced by water and air temperature, which implies that they could both be responding independently to changes in fjord circulation. Although data is not available for all years, the minimum front position is generally observed in late fall or in the winter indicating that calving continues after sea and air temperatures drop below freezing. It is therefore possible that the progressive buildup of sea

ice in the fjord is the main factor suppressing calving in the winter. Decreasing sea ice concentrations and earlier ice mélange clearing dates have the potential to significantly affect glacier retreat by lengthening the duration of the season over which strong calving occurs (Joughin *et al.*, 2008c; Christoffersen *et al.*, 2012; Joughin *et al.*, 2012; Walter *et al.*, 2012).

2.7 Conclusion

The timelapse dataset covering the terminus at Rink Isbræ allows for the detailed characterisation of calving activity and the identification of single events. Results show two distinct calving styles with different temporal and spatial footprints. Small magnitude events which tend to occur near the margins are concentrated in highly crevassed areas of the terminus where the ice is probably grounded. Events in this first category experience sudden increases in frequency immediately following ice mélange clearing and peak in July coinciding with maximum meltwater runoff. Their spatial distribution is correlated with the location of upwellings where submarine melt rates and undercutting are expected to be at their highest. It is suggested that events of low magnitudes occur in the fractured areas of the terminus where melt undercutting, and potentially hydrofracturing, destabilise the preexisting crevasses and lead to the frequent detachment of smaller icebergs. In winter, the presence of ice mélange is believed to prevent icebergs from drifting away from the already fractured front. It is suggested that closer to the margins the ice is too fractured to support the advance of a floating ice tongue. Those grounded areas are instead frequently eroded due to their sensitivity to melt and runoff. Although the impact of small events is limited in terms of scale and resulting mass loss, they play a crucial role in glacier dynamics by modifying front geometry.

The second calving style is characterised by the sporadic detachment of km-sized tabular icebergs which is not prevented by the presence of the ice mélange over the winter months. However, based on the current dataset, the yearly advance and retreat cycle suggests that ice mélange has a stabilising effect on terminus behaviour. Major calving events mainly affect the midsection of the front where deep water and higher ice velocities bring the ice margin towards floatation. It is

therefore suggested that the large full-depth calving events occur in response to mechanical forcing where failure and rift propagation are induced by longitudinal stretching and buoyant flexure. Due to their spatial extent the major events are responsible for most of the mass lost through calving and as a result they substantially modify front geometry. The seasonal growth and decay of the floating ice tongue and the associated variations in backstress are additionally believed to modify longitudinal stress gradients and cause the seasonal velocity variations (Howat *et al.*, 2010). The slight retreat ($\sim$ 700 m) and decreasing seasonal range between the maximum and minimum position observed over the study period, may potentially be explained by a change in terminus geometry. If the glacier thins below its floatation thickness and/or retreats into deeper water, increased buoyancy may result in increased calving rates. Buoyancy-driven positive feedbacks between calving and dynamic thinning therefore provide an effective mechanism for terminus retreat.

Overall the spatial and temporal variability of calving styles observed at Rink Isbræ seems to be related to terminus geometry including crevasse patterns, ice thickness and fjord topography. Longitudinal stretching as well as buoyancy conditions can be considered as the primary controls on terminus behaviour. Undercutting by submarine melt and hydrofracturing, both intensified by increased meltwater runoff, act as enhancing mechanisms. The backstress provided by the ice mélange is on the other hand a mitigating factor, limiting calving in the winter. The variability in calving behaviour emerging from the evidence reviewed in this study shows that Rink Isbræ experiences two different calving styles concurrently. It is suggested that the low magnitude events are melt-driven, whereas the major ones are mechanically-driven and occur mainly in response to buoyant-flexure. This clearly indicates that one single glacier can exhibit distinct calving styles resulting from the interaction between different calving mechanisms. As the mechanically-driven major calving events are responsible for most of the mass lost through calving at Rink, the same mechanism may also affect calving at other Greenland glaciers and therefore represent an important control on the stability of the ice sheet.

CONCLUSION

L'étude présentée dans le chapitre précédent offre un exemple de la variabilité dans les styles de vêlage observés aux termini des glaciers émissaires du Groenland. L'objectif était de documenter les événements de vêlage individuels à Rink Isbræ et de vérifier si une étude semi-qualitative permettait d'identifier les mécanismes de vêlage agissant au terminus. Un inconvénient majeur de la méthode utilisée est que le pas d'échantillonnage ne permet pas de déterminer si la perte d'une certaine quantité de glace à l'intérieur de la période de 24 h entre les images est le résultat d'un seul événement majeur, ou de plusieurs plus petits évènements. Il serait donc utile d'augmenter la fréquence des d'échantillonnages et d'acquérir par exemple des images toutes les heures pendant les périodes de forte activité de vêlage. Il serait aussi intéressant d'acquérir des images lors des mois d'hiver car, même si l'activité au front est réduite, Rink continue de produire de grands icebergs tabulaires qui ne sont malheureusement pas répertoriés.

L'étude de l'activité de vêlage à l'échelle des évènement individuels représente effectivement un défi. Plusieurs méthodes automatiques ont été utilisées pour détecter des événements de vêlage, y compris les techniques de photogrammétrie terrestre (O'Neel *et al.*, 2003; Ahn and Box, 2010; Chapuis *et al.*, 2010), le radar au sol (Rolstad and Norland, 2009; Chapuis *et al.*, 2010), la sismique passive (Qamar, 1988; O'Neel *et al.*, 2007, 2010; Tsai and Ekström, 2007; Amundson *et al.*, 2008, 2010; Richardson *et al.*, 2010; Köhler *et al.*, 2011), et les enregistrements acoustiques (Amundson *et al.*, 2010; Richardson *et al.*, 2010). Les observations visuelles directes permettent de surveiller continuellement le front (Washburn, 1936; Warren *et al.*, 1995; O'Neel *et al.*, 2003, 2007; Chapuis *et al.*, 2010; Chapuis and Tetzlaff, 2014) et peuvent fournir des données qualitatives supplémentaires concernant l'emplacement, l'ampleur et le timing des événements individuels. Chaque méthode a ses forces et inconvénients, mais elles permettent toutes d'obtenir une caractérisation détaillée des styles de vêlage et de leur variabilité temporelle et spatiale.

L'étude des styles de vêlage est utile car, comme dans le cas de Rink Isbræ, elle permet d'identifier les mécanismes modifiant la stabilité des glaciers émissaires. Compte tenu de la variabilité des processus observés d'un glacier à l'autre, des incertitudes demeurent quand à l'importance relative de chaque mécanisme et aux rétroactions qui les accompagnent. Les tentatives pour lier un comportement spécifique à un seul paramètre, comme la production d'eau de fonte, la fonte sous-marine, ou les concentrations de la glace de mer par exemple, sont la preuve de la nature complexe des processus de vêlage et de la dynamique glaciaire (Benn *et al.*, 2007b; Carr *et al.*, 2013). L'état actuel des connaissances concernant la dynamique des glaciers vêlants est principalement basé sur un petit nombre de glaciers largement étudiés qui ne représentent qu'un échantillon limité de la population totale. Bien que les glaciers situés dans des régions spécifiques tels que l'ouest du Groenland par exemple répondent de manière synchrone à certains forçages environnementaux, des différences significatives existent dans leurs comportements respectifs. Des études récentes menées sur les dernières décennies ont démontré que Rink Isbræ est resté relativement stable tandis que la majorité des glaciers de l'ouest du Groenland ont connu un amincissement, une augmentation de vélocité ainsi qu'un recul de leur terminus (Howat *et al.*, 2010; McFadden *et al.*, 2011). Ceci suggère que l'augmentation récente des températures de surface de l'air en été, ainsi que les températures de surface de l'océan ont eu peu d'effet sur Rink Isbræ et que les facteurs spécifiques au glacier tels que l'épaisseur de la marge et la topographie du fjord jouent un rôle important dans la médiation de la réponse du glacier aux variations climatiques (Howat *et al.*, 2010; McFadden *et al.*, 2011; Bevan *et al.*, 2012). Le rôle des facteurs spécifiques à chaque glacier dans la modulation de la dynamique glaciaire est crucial car ceux-ci peuvent avoir plus d'influence que les forçage climatique, et permettre à certains glaciers d'avancer dans une période où les conditions climatiques favorisent un retrait (Carr *et al.*, 2013). La présente étude a été menée sur un glacier relativement stable démontrant peu de variation de position terminale à long terme. Les conclusions obtenues représentent donc une contribution importante à l'étude des processus de vêlage dans des conditions stables, où la dynamique glaciaire n'est pas dominée par des conditions de recul rapide du terminus comme sur plusieurs autres glaciers au Groenland.

Les projections concernant la hausse des niveau marins au cours des deux prochains siècles prévoient que les processus de vêlage d'icebergs vont représenter la majorité de la contribution volumique des glaciers émissaires du Groenland (Nick *et al.*, 2013). En raison des incertitudes concernant les mécanismes responsables des variations des taux de vêlage, des études plus approfondies sont nécessaires pour déterminer comment les rétroactions entre les processus peuvent changer en réponse aux variations climatiques prévues pour les prochains siècles, et comment ceux-ci peuvent influencer la stabilité des glaciers émissaires et de la calotte glaciaire du Groenland.

RÉFÉRENCES

Ahn, Y. and Box, J. E. (2010). Glacier velocities from time-lapse photos: technique development and first results from the Extreme Ice Survey (EIS) in Greenland. *Journal of Glaciology*, *56*(198), 723–734.

Amundson, J. M., Fahnestock, M., Truffer, M., Brown, J., Lüthi, M. P. and Motyka, R. J. (2010). Ice mélange dynamics and implications for terminus stability, Jakobshavn Isbræ, Greenland. *Journal of Geophysical Research*, *115*(F01005).

Amundson, J. M., Truffer, M., Lüthi, M. P., Fahnestock, M., West, M. and Motyka, R. J. (2008). Glacier fjord, and seismic response to recent large calving events, Jakobshavn Isbræ, Greenland. *Geophysical Research Letters*, *35*(L22501).

Arendt, A. A., Echelmeyer, K. A., Harrison, W. D., Lingle, C. S. and Valentine, V. B. (2002). Rapid wastage of Alaska glaciers and their contribution to rising sea level. *Science*, *297*, 382–386.

Bamber, J. L., Alley, R. B. and Joughin, I. (2007). Rapid response of modern day ice sheets to external forcing. *Earth and Planetary Science Letters*, *257*, 1–13.

Bassis, J. N. (2011). The statistical physics of iceberg calving and the emergence of universal calving laws. *Journal of Glaciology*, *57*(201), 3–16.

Bassis, J. N. and Jacobs, S. (2013). Diverse calving patterns linked to glacier geometry. *Nature Geoscience*, *6*, 833–836.

Benn, D. I. and Evans, D. J. A. (2010). *Glaciers and glaciation* (2nd ed.). London: Hodder Education.

Benn, D. I., Hulton, N. R. J. and Mottram, R. H. (2007a). 'Calving laws', 'sliding laws' and the stability of tidewater glaciers. *Annals of Glaciology*, *46*, 123–130.

Benn, D. I., Warren, C. R. and Mottram, R. H. (2007b). Calving processes and the dynamics of calving glaciers. *Earth-Science Reviews*, *82*, 143–179.

Benn, D. I., Wiseman, S. and Hands, K. A. (2001). Growth and drainage of supraglacial lakes on debris-mantled Ngozumpa Glacier, Khumbu Himal, Nepal. *Journal of Glaciology*, *47*(159), 626–638.

Bevan, S. L., Luckman, A. J. and Murray, T. (2012). Glacier dynamics over the last quarter of a century at Helheim, Kangerdlugssuaq and 14 other major Greenland outlet glaciers. *The Cryosphere*, *6*, 923–937.

Box, J. E. and Decker, D. T. (2011). Greenland marine-terminating glacier area changes: 2000- 2010. *Annals of Glaciology*, *52*(59), 91–98.

Boyce, E. S., Motyka, R. J. and Truffer, M. (2007). Flotation and retreat of a lake-calving terminus, Mendenhall Glacier, southeast Alaska, USA. *Journal of Glaciology*, *53*(181), 211–224.

Brown, C. S., Meier, M. F. and Post, A. (1982). Calving speed of Alaska tidewater glaciers, with application to Columbia Glacier. *USGS Professional Paper*, *1258-C*.

Cappelen, J. e. (2014). Weather and climate data from greenland 1958-2013. *DMI Technical Report*, *14-08*.

Carr, J. R., Stokes, C. R. and Vieli, A. (2013). Recent progress in understanding marine-terminating Arctic outlet glacier response to climatic and oceanic forcing: Twenty years of rapid change. *Progress in Physical Geography*, *37*(4), 436–467.

Cassotto, R., Fahnestock, M., Amundson, J. M., Truffer, M. and Joughin, I. (2015). Seasonal and interannual variations in ice melange and its impact on terminus stability, Jakobshavn Isbræ, Greenland. *Journal of Glaciology*, *61*(225), 76–88.

Chapuis, A., Rolstad, C. and Norland, R. (2010). Interpretation of amplitude data from a ground-based radar in combination with terrestrial photogrammetry and visual observations for calving monitoring of Kronebreen, Svalbard. *Annals of Glaciology*, *51*(55), 34–40.

Chapuis, A. and Tetzlaff, T. (2014). The variability of tidewater-glacier calving: origin of event-size and interval distributions. *Journal of Glaciology*, *60*(222), 622–634.

Chauché, N., Hubbard, A., Gascard, J.-C., Box, J. E., Bates, R., Koppes, M., Sole, A., Christoffersen, P. and Patton, H. (2014). Ice-ocean interaction and calving front morphology at two west Greenland tidewater outlet glaciers. *The Cryosphere*, *8*, 1457–1468.

Christoffersen, P., O'Leary, M., van Angelen, J. H. and van den Broeke, M. (2012). Partitioning effects from ocean and atmosphere on the calving stability of Kangerdlugssuaq Glacier, East Greenland. *Annals of Glaciology*, *53*(60), 249–256.

Cook, A. J., Fox, A. J., Vaughan, D. G. and Ferrigno, J. G. (2005). Retreating glacier fronts on the Antarctic Peninsula over the past half-century. *Science*, *308*, 541–544.

Cook, S., Rutt, I. C., Murray, T., Luckman, A., Zwinger, T., Selmes, N., Goldsack, A. and James, T. D. (2014). Modelling environmental influences on calving at Helheim Glacier in eastern Greenland. *The Cryosphere*, *8*, 827–841.

Cook, S., Zwinger, T., Rutt, I. C., O'Neel, S. and Murray, T. (2012). Testing the effect of water in crevasses on a physically based calving model. *Annals of Glaciology*, *53*(60), 90–96.

Dowdeswell, J. A., Hogan, K. A., Cofaigh, C. Ó., Fugelli, E. M. G., Evans, J. and Noormets, R. (2014). Late Quaternary ice flow in a West Greenland fjord and cross-shelf trough system: submarine landforms from Rink Isbrae to Uummannaq shelf and slope. *Quaternary Science Reviews*, *92*, 292–309.

Dykes, R. C., Brook, M. S. and Winkler, S. (2010). The contemporary retreat of Tasman Glacier, Southern Alps, New Zealand, and the evolution of Tasman proglacial lake since AD 2000. *Erdkunde*, *64*(2), 141–154.

Enderlin, E. N. and Howat, I. M. (2013). Submarine melt rates estimates for floating termini of Greenland outlet glaciers (2000-2010). *Journal of Glaciology*, *59*(213), 67–75.

Hanson, B. and Hooke, LeB, R. (2000). Glacier calving: a numerical model of forces in the calving-speed/water-depth relation. *Journal of Glaciology*, *46*(153), 188–196.

Haresign, E. C. and Warren, C. R. (2005). Melt rates at calving termini: a study at Glaciar León, Chilean Patagonia. In C. Harris and J. B. Murton (dir.), *Cryospheric systems: glaciers and permafrost*, volume 242 99–110. London: Geological Society Special Publication.

Herdes, E., Copland, L., Danielson, B. and Sharp, M. (2012). Relationships between iceberg plumes and sea-ice conditions on northeast Devon Ice Cap, Nunavut, Canada. *Annals of Glaciology*, *53*(60), 1–9.

Howat, I. M., Box, J. E., Ahn, Y., Herrington, A. and McFadden, E. M. (2010). Seasonal variability in the dynamics of marine-terminating outlet glaciers in greenland. *Journal of Glaciology*, *56*(198), 601–613.

Howat, I. M. and Eddy, A. (2011). Multi-decadal retreat of Greenland's marine-terminating glaciers. *Journal of Glaciology*, *57*(203), 389–396.

Howat, I. M., Joughin, I., Fahnestock, M., Smith, B. E. and Scambos, T. A. (2008). Synchronous retreat and acceleration of southeast Greenland glaciers 2000-06: ice dynamics and coupling to climate. *Journal of Glaciology*, *54*(187), 646–660.

Howat, I. M., Joughin, I. and Scambos, T. A. (2007). Rapid changes in ice discharge from Greenland outlet glaciers. *Science*, *315*, 1559–1561.

Howat, I. M., Joughin, I., Tulaczyk, S. and Gogineni, S. (2005). Rapid retreat and acceleration of Helheim Glacier, east Greenland. *Geophysical Research Letters*, *32*(L22502).

James, T. D., Murray, T., Selmes, N., Scharrer, K. and O'Leary, M. (2014). Buoyant flexure and basal crevassing in dynamic mass loss at Helheim Glacier. *Nature Geoscience*, *7*, 593–596.

Jenkins, A. (2011). Convection-driven melting near the grounding lines of ice shelves and tidewater glaciers. *Journal of Physical Oceanography*, *41*(12), 2279–2294.

Joughin, I., Abdalati, W. and Fahnestock, M. (2004). Large fluctuations in speed on Greenland's Jakobshavn Isbræe glacier. *Nature*, *432*, 608–610.

Joughin, I., Alley, R. B. and Holland, D. M. (2012). Ice-sheet response to oceanic forcing. *Science*, *338*, 1172–1176.

Joughin, I., Das, S. B., King, M. A., Smith, B. E., Howat, I. M. and Moon, T. (2008a). Seasonal speedup along the western flank of the Greenland Ice Sheet. *Science*, *320*, 781–783.

Joughin, I., Howat, I., Alley, R. B., Ekstrom, G., Fahnestock, M., Moon, T., Nettles, M., Truffer, M. and Tsai, V. C. (2008b). Ice-front variation and tidewater behaviour on Helheim and Kangerdlugssuaq Glaciers, Greenland. *Journal of Geophysical Research*, *113*(F01004).

Joughin, I., Howat, I. M., Fahnestock, M., Smith, B., Krabil, W., Alley, R. B., Stern, H. and Truffer, M. (2008c). Continued evolution of Jakobshavn Isbræ following its rapid speedup. *Journal of Geophysical Research*, *113*(F04006).

Kirkbride, M. P. and Warren, C. R. (1997). Calving processes at a grounded ice cliff. *Annals of Glaciology*, *24*, 116–121.

Köhler, A., Chapuis, A., Nuth, C., Kohler, J. and Weidle, C. (2011). Seasonal variations of glacier dynamics at Kronebreen, Svalbard, revealed by calving related seismicity. *The Cryosphere Discussions*, *5*, 3291–3321.

Krimmel, R. M. (2001). Photogrammetric data set, 1957-2000, and bathymetric measurements for Columbia Glacier, Alaska. *USGS Water-Resources Investigations Report 01-4089.*

Luckman, A. and Murray, T. (2005). Seasonal variation in velocity before retreat of Jakobshavn Isbræ, Greenland. *Geophysical Research Letters, 32*(L08501). http://dx.doi.org/10.1029/2005GL022519

MacAyeal, D. R., Scambos, T. A., Hulbe, C. L. and Fahnestock, M. A. (2003). Catastrophic ice-shelf break-up by an ice-shelf-fragment-capsize mechanism. *Journal of Glaciology, 49*(164), 22–36.

McFadden, E. M., Howat, I. M., Joughin, I., Smith, B. E. and Ahn, Y. (2011). Changes in the dynamics of marine terminating outlet glaciers in west Greenland (2000-2009). *Journal of Geophysical Research, 116*(F02022).

Meier, M. F. and Post, A. (1987). Fast tidewater glaciers. *Journal of Geophysical Research, 92*(B9), 9051–9058.

Meier, M. F., Rasmussen, L. A., Krimmel, R. M., Olsen, R. W. and Frank, D. (1985). Photogrammetric determination of surface altitude, terminus position, and ice velocity of Columbia Glacier, Alaska. *USGS Professional Paper, 1258-F.*

Moon, T. and Joughin, I. (2008). Changes in ice front position of Greenland's outlet glaciers from 1992 to 2007. *Journal of Geophysical Research, 113*(F02022).

Motyka, R. J. (1997). Deep-water calving at Le Conte Glacier, Southeast Alaska. In C. J. van der Veen (dir.). *Calving glaciers: Report of a workshop, Feb. 28-March 2, 1997, Report 15*, 115–118., Ohio State University, Columbus. Byrd Polar Research Centre.

Motyka, R. J., Hunter, L., Echelmeyer, K. A. and Connor, C. (2003). Submarine melting at the terminus of a temperate tidewater glacier, LeConte Glacier, Alaska, USA. *Annals of Glaciology, 36*, 57–65.

Motyka, R. J., Truffer, M., Fahnestock, M., Mortensen, J., Rysgaard, S. and Howat, I. (2011). Submarine melting of the 1985 Jakobshavn Isbræ floating

tongue and the triggering of the current retreat. *Journal of Geophysical Research, 116*(F01007).

Münchow, A., Padman, L. and Fricker, H. A. (2014). Interannual changes of the floating ice shelf of Petermann Gletscher, North Greenland, from 2000 to 2012. *Journal of Glaciology, 60*(221), 489–499.

Murray, T., Scharrer, K., James, T. D., Dye, S. R., Hanna, E., Booth, A. D., Selmes, N., Luckman, A., Hughes, A. L. C., Cook, S. and Huybrechts, P. (2010). Ocean regulation hypothesis for glacier dynamics in southeast Greenland and implications for ice sheet mass changes. *Journal of Geophysical Research, 115*(F03026).

Nettles, M., Larsen, T. B., Elósegui, P., Hamilton, G. S., Stearns, L. A., Ahlstrøm, A. P., Davis, J. L., Andersen, M. L., de Juan, J., Khan, S. A., Stenseng, L., Ekström, G. and Forsberg, R. (2008). Step-wise changes in glacier flow speed coincide with calving and glacial earthquakes at Helheim Glacier, Greenland. *Geophysical Research Letters, 35*(L24503).

Nick, F. M., van der Veen, C. J., Vieli, A. and Benn, D. I. (2010). A physically based calving model applied to marine outlet glaciers and implications for the glacier dynamics. *Journal of Glaciology, 56*(199), 781–794.

Nick, F. M., Vieli, A., Andersen, M. L., Joughin, I., Payne, A., Edwards, T. L., Pattyn, F. and van de Wal, R. S. W. (2013). Future sea-level rise from Greenland's main outlet glaciers in a warming climate. *Nature, 497*, 235–238.

Nick, F. M., Vieli, A., Howat, I. M. and Joughin, I. (2009). Large-scale changes in Greenland outlet glacier dynamics triggered at the terminus. *Nature Geoscience, 2*, 110–114.

Oerlemans, J. (2005). Extracting a climate signal from 169 glacier records. *Science, 308*, 675–677.

O'Leary, M. and Christoffersen, P. (2013). Calving on tidewater glaciers amplified by submarine frontal melting. *The Cryosphere, 7*, 119–128.

O'Neel, S., Echelmeyer, K. A. and Motyka, R. J. (2001). Short-term flow dynamics of a retreating tidewater glacier: LeConte Glacier, Alaska, USA. *Journal of Glaciology*, *47*(159), 567–578.

O'Neel, S., Echelmeyer, K. A. and Motyka, R. J. (2003). Short-term variations in calving of a tidewater glacier: LeConte Glacier, Alaska, USA. *Journal of Glaciology*, *49*(167), 587–598.

O'Neel, S., Lasen, C. F., Rupert, N. and Hansen, R. (2010). Iceberg calving as a primary source of regional-scale glacier-generated seismicity in the St. Elias Mountains, Alaska. *Journal of Geophysical Research*, *115*(F04034).

O'Neel, S., Marshall, H. P., McNamara, D. E. and Pfeffer, W. T. (2007). Seismic detection and analysis of icequakes at Columbia Glacier, Alaska. *Journal of Geophysical Research*, *112*(F03S23).

O'Neel, S., Pfeffer, W. T., Krimmel, R. and Meier, M. (2005). Evolving force balance at Columbia Glacier, Alaska, during its rapid retreat. *Journal of Geophysical Research*, *110*(F03012).

Pelto, M. S. and Warren, C. R. (1991). Relationship between tidewater glacier calving velocity and water depth at the calving front. *Annals of Glaciology*, *15*, 115–118.

Pfeffer, W. T. (2007). A simple mechanism for irreversible tidewater glacier retreat. *Journal of Geophysical Research*, *112*(F03S25).

Post, A. (1975). Preliminary hydrology and historic terminal changes of Columbia Glacier, Alaska. *USGS Hydrologic Investigations Atlas*, *Ha-559*, 3 sheets, scale 1:20,000.

Post, A., O'Neel, S., Motyka, R. J. and Streveler, G. (2011). A complex relationship between calving glaciers and climate. *Eos Transactions American Geophysical Union*, *92*(37), 305–307.

Qamar, A. (1988). Calving icebergs: A source of low-frequency seismic signals from Columbia Glacier, Alaska. *Journal of Geophysical Research*, *93*(B6), 6615–6623.

Reeh, N., Højmark Thomsen, H., Higgins, A. K. and Weidick, A. (2001). Sea ice and the stability of north and northeast Greenland floating glaciers. *Annals of Glaciology, 33*, 474–480.

Richardson, J. P., Waite, G. P., FitzGerald, K. A. and Pennington, W. D. (2010). Characteristics of seismic and acoustic signals produced by calving, Bering Glacier, Alaska. *Geophysical Research Letters, 37*(L03503).

Rignot, E. and Kanagaratnam, P. (2006). Changes in the velocity structure of the Greenland Ice Sheet. *Science, 311*, 986–990.

Rignot, E., Kopped, M. and Velicogna, I. (2010). Rapid submarine melting of the calving faces of West Greenland glaciers. *Nature Geoscience, 3*, 187–191.

Rignot, E., Rivera, A. and Casassa, G. (2003). Contribution of the Patagonia Icefields of South America to sea level rise. *Science, 302*, 434–437.

Rignot, E., Velicogna, I., van den Broeke, M. R., Monaghan, A. and Lenaerts, J. (2011). Acceleration of the contribution of the Greenland and Antarctic ice sheets to sea level rise. *Geophysical Research Letters, 38*(L05503).

Röhl, L. (2006). Thermo-erosional notch development at fresh-water-calving Tasman Glacier, New Zealand. *Journal of Glaciology, 52*(177), 203–213.

Rolstad, C. and Norland, R. (2009). Ground-based interferometric radar for velocity and calving-rate measurements of the tidewater glacier at Kronebreen, Svalbard. *Annals of Glaciology, 50*, 47–54.

Scambos, T. A., Hulbe, C., Fahnestock, M. and Bohlander, J. (2000). The link between climate warming and break-up of ice shelves in the Antarctic Peninsula. *Journal of Glaciology, 46*(154), 516–530.

Schild, K. M. and Hamilton, G. S. (2013). Seasonal variations of outlet glacier terminus position in Greenland. *Journal of Glaciology, 59*(216), 759–770.

Sciascia, R., Straneo, F., Cenedese, C. and Heimback, P. (2013). Seasonal variability of submarine melt rate and circulation in an East Greenland fjord. *Journal of Geophysical Research: Oceans, 118*, 2492–2506.

Seale, A., Christoffersen, P., Mugford, R. I. and O'Leary, M. (2011). Ocean forcing of the greenland ice sheet: Calving fronts and patterns of retreat identified by automatic satellite monitoring of eastern outlet glaciers. *Journal of Geophysical Research*, *116*(D02013).

Skvarca, P., Raup, B. and De Angelis, H. (2003). Recent behaviour of Glacial Upsala, a fast-flowing calving glacier in Lago Argentino, southern Patagonia. *Annals of Glaciology*, *36*, 184–188.

Sohn, H. G., Jezek, K. C. and van der Veen, C. J. (1998). Jakobshavn Glacier, West Greenland: 30 years of spaceborne observations. *Geophysical Research Letters*, *25*(14), 2699–2702.

Straneo, F., Curry, R. G., Sutherland, D. A., Hamilton, G. S., Cenedese, C., Våge, K. and Stearns, L. A. (2011). Impact of fjord dynamics and glacial runoff on the circulation near Helheim Glacier. *Nature Geoscience*, *4*, 322–327.

Straneo, F., Hamilton, G. S., Sutherland, D. A., Stearns, L. A., Davidson, F., Hammill, M. O., Stenson, G. B. and Rosing-Asvid, A. (2010). Rapid circulation of warm subtropical waters in a major glacial fjord in East Greenland. *Nature Geoscience*, *3*, 182–186.

Theakstone, W. H. and Knudsen, N. T. (1986). Recent changes of a calving glacier, Austerdalsisen, Svartisen, Norway. *Geografiska Annaler*, *68*(4), 303–316.

Thomas, R. H. (2004). Force-perturbation analysis of recent thinning and acceleration of Jakobshavn Isbræ, Greenland. *Journal of Glaciology*, *50*(168), 57–66.

Tsai, V. C. and Ekström, G. (2007). Analysis of glacial earthquakes. *Journal of Geophysical Research*, *112*(F03S22).

van der Veen, C. J. (1996). Tidewater calving. *Journal of Glaciology*, *42*(141), 375–385.

van der Veen, C. J. (1997a). Backstress: what it is and how it affects glacier flow. In C. J. van der Veen (dir.). *Calving glaciers: Report of a workshop, Feb.*

28-March 2, 1997, Report 15, 173–180., Ohio State University, Columbus. Byrd Polar Research Centre.

van der Veen, C. J. (1997b). Controls on the position of iceberg-calving fronts. In C. J. van der Veen (dir.). *Calving glaciers: Report of a workshop, Feb. 28-March 2, 1997, Report 15*, 163–172., Ohio State University, Columbus. Byrd Polar Research Centre.

van der Veen, C. J. (1998). Fracture mechanics approach to penetration of surface crevasses on glaciers. *Cold Regions Science and Technology, 27*, 31–47.

van der Veen, C. J. (2002). Calving glaciers. *Progress in Physical Geography, 26*(1), 96–122.

van der Veen, C. J. (2007). Fracture propagation as means of rapidly transferring surface meltwater to the base of glaciers. *Geophysical Research Letters, 34*(L01501).

Vieli, A., Funk, M. and Blatter, H. (2000). Tidewater glaciers: frontal flow acceleration and basal sliding. *Annals of Glaciology, 31*, 217–221.

Vieli, A., Funk, M. and Blatter, H. (2001). Flow dynamics of tidewater glaciers: a numerical modelling approach. *Journal of Glaciology, 47*(159), 595–606.

Vieli, A., Jania, J., Blatter, H. and Funk, M. (2004). Short-term velocity variations on Hansbreen, a tidewater glacier in Spitsbergen. *Journal of Glaciology, 50*(170), 389–398.

Vieli, A., Jania, J. and Kolondra, L. (2002). The retreat of a tidewater glacier: observations and model calculations on Hansbreen, Spitsbergen. *Journal of Glaciology, 48*(163), 592–600.

Vieli, A. and Nick, F. M. (2011). Understanding and modelling rapid dynamic changes of tidewater outlet glaciers: Issues and implications. *Surveys in Geophysics, 32*, 437–458.

Walter, F., O'Neel, S., McNamara, D., Pfeffer, W. T. and Bassis, J. N. (2010). Iceberg calving during transition from grounded to floating ice: Columbia Glacier, Alaska. *Geophysical Research Letters, 37*(L15501).

Walter, J. I., Box, J. E., Tulaczyk, S., Brosky, E. E., Howat, I. M., Ahn, Y. and Brown, A. (2012). Oceanic mechanical forcing of a marine-terminating Greenland glacier. *Annals of Glaciology*, *53*(60), 181–192.

Warren, C., Benn, D., Winchester, V. and Harrison, S. (2001). Buoyancy-driven lacustrine calving, Glaciar Nef, Chilean Patagonia. *Journal of Glaciology*, *47*(156), 135–146.

Warren, C. R., Glasser, N. F., Harrison, S., Winchester, V., Kerr, A. R. and Rivera, A. (1995). Characteristics of tide-water calving at Glaciar San Rafael, Chile. *Journal of Glaciology*, *41*(138), 273–289.

Washburn, Jr, H. B. (1936). The Harvard Dartmouth Alaskan expeditions, 1933-1934. *The Geographical Journal*, *87*(6), 481–493.

Xu, Y., Rignot, E., Menemenlis, S. and Koppes, M. (2012). Numerical experiments on subaqueous melting of Greenland tidewater glaciers in response to ocean warming and enhanced subglacial discharge. *Annals of Glaciology*, *53*(60), 229–234.